



Definitions and methods to estimate regional land carbon fluxes for the second phase of the REgional Carbon Cycle Assessment and Processes Project (RECCAP-2)

Philippe Ciais¹, Ana Bastos², Frédéric Chevallier¹, Ronny Lauerwald^{1,3}, Ben Poulter⁴, Pep Canadell⁵,
5 Gustaf Hugelius^{6,7}, Robert B. Jackson⁸, Atul Jain⁹, Matthew Jones¹⁰, Masayuki Kondo¹¹, Ingrid T.
Luijkx¹², Prabir K Patra¹³, Wouter Peters^{12,14}, Julia Pongratz¹⁵, A. M. Roxana Petrescu¹⁶, Shilong
Piao^{17,18}, Chunjing Qiu¹, C. Von Randow¹⁹, Pierre Regnier³, Marielle Saunois¹, Robert Scholes²⁰, A.
Shvidenko^{21,22}, Hanqin Tian²³, Hui Yang¹, Xuhui Wang¹⁷ and Bo Zheng¹

¹ Laboratoire des Sciences du Climat et de l'Environnement, CEA-CNRS-UVSQ-U.P.Saclay, Gif sur Yvette, France

10 ² Max-Planck-Institut für Biogeochemie, Hans-Knöll-Str. 10, 07745, Jena, Germany

³ Université Libre de Bruxelles, Department Geoscience, Environment & Society, Bruxelles, Belgium

⁴ NASA Goddard Space Flight Center, Biospheric Sciences Lab., Greenbelt, USA

⁵ Global Carbon Project, CSIRO Oceans and Atmosphere, GPO Box 1700, Canberra, Australia

⁶ Department of Physical Geography, Stockholm University, Sweden

15 ⁷ Bolin Centre for Climate Research, Stockholm University, Sweden

⁸ Department of Earth System Science, Woods Institute for the Environment, and Precourt Institute for Energy, Stanford University, USA

⁹ Department of Atmospheric Sciences, University of Illinois, Urbana, IL 61821, USA

20 ¹⁰ Tyndall Centre for Climate Change Research, School of Environmental Sciences, University of East Anglia, Norwich Research Park, Norwich NR4 7TJ, UK

¹¹ Center for Global Environmental Research, National Institute for Environmental Studies, Tsukuba, Japan

¹² Meteorology and Air Quality, Wageningen University, Wageningen, the Netherlands

¹³ Japan Agency for Marine-Earth Science and Technology (JAMSTEC), Yokohama, Japan

¹⁴ Centre for Isotope Research, University of Groningen, Groningen, the Netherlands

25 ¹⁵ Department für Geographie, Ludwig-Maximilians-Universität München, Luisenstr. 37, München, Germany

¹⁶ Department of Earth Sciences, Vrije Universiteit Amsterdam, Amsterdam, the Netherlands

¹⁷ Sino-French Institute for Earth System Science, College of Urban and Environmental Sciences, Peking University, Beijing, China

¹⁸ Institute of Tibetan Plateau Research, Chinese Academy of Sciences, Beijing 100085, China

30 ¹⁹ Earth System Science Center, National Institute of Space Research, Brazil

²⁰ Global Change Institute, University of the Witwatersrand, Johannesburg, South Africa

²¹ International Institute for Applied Systems Analysis, A-2361 Laxenburg Austria

²² Center of Productivity of Forests Russian Academy of Sciences, Moscow, Russia

35 ²³ International Center for Climate and Global Change Research, School of Forestry and Wildlife Sciences, Auburn University, Auburn, USA

Correspondence to: Philippe Ciais (philippe.ciais@lsce.ipsl.fr)



40 **Abstract.**

Regional land carbon budgets provide insights on the spatial distribution of the land uptake of atmospheric carbon dioxide, and can be used to evaluate carbon cycle models and to define baselines for land-based additional mitigation efforts. The scientific community has been involved in providing observation-based estimates of regional carbon budgets either by
45 downscaling atmospheric CO₂ observations into surface fluxes with atmospheric inversions, by using inventories of carbon stock changes in terrestrial ecosystems, by upscaling local field observations such as flux towers with gridded climate and remote sensing fields or by integrating data-driven or process-oriented terrestrial carbon cycle models. The first coordinated attempt to collect regional carbon budgets for nine regions covering the entire globe in the RECCAP-1 project has delivered estimates for the decade 2000-2009, but these budgets were not comparable between regions, due to different definitions and
50 component fluxes reported or omitted. The recent recognition of lateral fluxes of carbon by human activities and rivers, that connect CO₂ uptake in one area with its release in another also requires better definition and protocols to reach harmonized regional budgets that can be summed up to the globe and compared with the atmospheric CO₂ growth rate and inversion results. In this study, for the international initiative RECCAP-2 coordinated by the Global Carbon Project, which aims as an update of regional carbon budgets over the last two decades based on observations, for 10 regions covering the globe, with a
55 better harmonization than the precursor project, we provide recommendations for using atmospheric inversions results to match bottom-up carbon accounting and models, and we define the different component fluxes of the net land atmosphere carbon exchange that should be reported by each research group in charge of each region. Special attention is given to lateral fluxes, inland water fluxes and land use fluxes.

60 **Introduction**

The objective of this paper is to define the land-atmosphere CO₂ or total carbon (C) fluxes to be used in the REgional Carbon Cycle Assessment and Processes-2 (RECCAP2) project. Accurate and consistent observation-based estimates terrestrial carbon budgets at regional scales are needed to understand the global land carbon sink, to evaluate land carbon models used for carbon
65 budget assessments and future climate projections, and to define baselines for land-based mitigation efforts. In the previous synthesis called RECCAP1, regional data from inventories were compared with global models output from atmospheric inversions, process-based land models, the results being synthesized in a special issue (https://bg.copernicus.org/articles/special_issue107.html) for 9 land regions in the period 2000-2009. The definition of fluxes was not harmonized and inland waters and trade induced CO₂ fluxes were not considered for most regions. The RECCAP1
70 synthesis spurred efforts to provide new global analysis of inland water CO₂ fluxes (Raymond et al. 2013). Recently, Ciais et al. (2020) collected bottom up inventory estimates from RECCAP1 papers and completed them with other components, to derive the first global bottom up estimate of the net land atmosphere C exchange, that compared well with the independent top down estimate obtained from the CO₂ growth rate minus fossil fuel emissions and ocean uptake.



75 The aims of RECCAP2 are to collect and synthesize regional CO₂, CH₄ and N₂O budgets for 10 continental-scale regions (including one ‘cross cutting’ region consisting of all permafrost covered boreal areas), together covering the globe (Fig. 1). There is thus a requirement for harmonization and consistency, sufficient to be able to scale regional budgets to the globe and to compare different regions with each other for all component fluxes and each greenhouse gas. There is further an intention to compare the results of top-down atmospheric inversions with bottom-up accounting approaches. Since research groups
80 working on the synthesis of greenhouse gas budgets in different regions or using different approaches use different datasets and definitions, it is important to provide a set of shared and agreed definitions that are as precise as possible for each flux to be reported. We focus here on land C and CO₂ budgets, defined from two approaches: ‘top-down’ estimates from atmospheric inversions, and; ‘bottom-up’ carbon accounting approaches based on C stock inventories, process- and data-oriented models.

85 Atmospheric inversions analysis of land-atmosphere CO₂ fluxes inherently differs from bottom-up C budgets for two reasons. The first one is the existence of lateral fluxes at the land surface and from the land to the ocean, which displace carbon initially fixed as CO₂ from the atmosphere in one region and release it outside that region. Consequently, the CO₂ flux diagnosed by an inversion is not equal to the change of stock in a region. The second one is that carbon enters from the atmosphere in the land reservoirs almost uniquely as CO₂ fixed by photosynthesis, while it is released both as CO₂ and as reduced carbon
90 compounds encompassing CO, CH₄ and biogenic volatile organic compounds (BVOCs). Again, this process makes CO₂ fluxes different from total carbon fluxes across the land-atmosphere surface.

To address these issues, Section 1 of this paper covers atmospheric CO₂ inversions and the treatment of reduced C compounds emissions, with the goal to make inversion results comparable with total C flux estimates from bottom-up approaches. Section
95 2 deals with bottom up estimates and provides definitions of the main component land-atmosphere C fluxes that should be estimated individually to provide a full assessment of the C balance of each region, to enable consistent comparisons between regions and upscaling of regional budgets to the globe. Section 3 provides a description of different approaches used to derive regional component C fluxes in different bottom-up approaches, outlining which fluxes are included or ignored by each different approach. Section 4 gives recommendations regarding the estimation of carbon emissions resulting from land use
100 change, with systematic errors and omission errors associated to different approaches. We conclude by providing recommendations for a multiple-tier approach to develop regional C budgets in RECCAP2.

1 Top-down land-atmosphere C fluxes from atmospheric inversions

1.1 Land CO₂ fluxes covered by inversions

The approaches known as top-down atmospheric inversions estimate the net CO₂ flux exchanged between the surface and the
105 atmosphere by using atmospheric transport models and CO₂ mole fraction measurements at various locations. The mole



fraction data comes from surface stations, which have been available in increasing numbers since 1957. More recently, total column mole fraction of CO₂ have been observed with global coverage by satellites, GOSAT since 2009 and OCO-2 since 2014 (Liu et al., 2020). Because the sampling of the atmosphere is sparse, even with the recent global satellite observations, there is an infinite number of flux combinations that can fit atmospheric CO₂ observations within their errors. Most inversions therefore use a Bayesian statistical approach where an optimal CO₂ flux is found as a maximum likelihood estimate in the statistical distribution of possible fluxes, given a prior value and its uncertainty distribution, and observations, which also have an uncertainty distribution. The effect of fossil fuel and cement production CO₂ emissions (hereafter collectively called “fossil fuel” for simplicity) on mixing ratios gradients is accounted for by prescribing transport models with an assumed fixed map of fossil CO₂ emissions. The signal from these emissions in the space of concentrations is removed at pre- or post-processing stage from inversions to solve for residual non-fossil CO₂ fluxes. Over land, output fluxes from inversions are thus the sum of all non-fossil CO₂ fluxes. This includes gross primary production CO₂ uptake, plant and soil respiration, litter photo-oxidation, biomass-burning emissions both from wildfires and for the purposes of energy provision, inland-water fluxes, the oxidative release of CO₂ from biomass consumed by animals and humans and decaying in waste pools, CO₂ emitted by insect grazing, geological CO₂ emissions from volcanoes and seepage from below-ground sources, CO₂ uptake from weathering reactions and geological CO₂ release from microbial oxidation of petrogenic carbon (Hemingway et al., 2018). Inversions have very limited capability to separate those different fluxes unless they use additional information, which is not the case for inversions used in global budgets. An example of additional information is the use of CO as a tracer, to separate emissions from vegetation fires from those from fossil fuels and respiration.

1.2 Prescribing fossil CO₂ emission fields, inclusive of bunker fuels

Within RECCAP1 (Canadell et al., 2015), the same fossil fuel emission estimate was subtracted from the total posterior fluxes of participating inversions, even when those inversions had used different fossil fuel inventories (Peylin et al., 2013). This inconsistency between the inversion process and the inversion post-processing induced artifacts (see discussion in Thompson et al., 2016) but is of lesser importance for the inter-comparison than the use of different fossil fuel inventories within the inversion ensemble. We thus recommend here that a standard gridded a priori fossil fuel CO₂ emission estimate is used by all regions in RECCAP2, such as recently prepared by Jones et al. (2020). Another important issue is that about 10% of CO₂ emissions come from mobile sources from ships at the ocean surface, and aircraft in the volume of the atmosphere. We recommend that these ‘bunker fuel’ emissions are prescribed to RECCAP2 inversions in using three-dimensional maps of fossil fuel CO₂ emissions. Each grid box should thus include the emissions within its borders, along ship routes on the surface, and flight paths at the appropriate altitude in the atmosphere. This option is increasingly viable due to the emerging availability of sectoral emissions grids for recent years (Choulga et al., 2020; Jones et al., 2020).



1.3 Reduced-C compounds emissions

Reduced-C compounds are emitted by the land surface as biogenic and anthropogenic CH₄, BVOCs and CO. Globally, emissions of reduced C compounds from land ecosystems and fossil fuel use are a large and overlooked component of the C budget, with CO-carbon emissions from incomplete fuel combustion equaling $\approx 0.3 \text{ PgC y}^{-1}$ (Zheng et al., 2019), CH₄-carbon emissions 0.43 PgC y^{-1} (Saunois et al., 2020) and non-methane biogenic compounds emissions up to 0.75 PgC y^{-1} (Sindelarova et al., 2014). Given that inversions only assimilate atmospheric observations of CO₂, they omit regional emissions of reduced C compounds. However, reduced C compounds all oxidize to CO₂ in the atmosphere, with lifetimes of hours to days for BVOCs, months for CO and nearly ten years for CH₄. The global CO₂ growth rate thus includes the signal of the global reduced C emissions being oxidized into CO₂ in the volume of the atmosphere, though not necessarily in the year of their emission. By fitting the global CO₂ growth rate, inversions thus include global emission of reduced C compounds, which is diagnosed as a diffuse natural CO₂ emission over the whole surface of the globe, in that year. This implies that inversions place a wrong ocean CO₂ emission in the place of reduced C compounds emitted only over land (Enting and Mansbridge, 1991). Further, current inversions assume that all the fossil C is emitted as CO₂ ignoring incomplete fuel combustion emitted as CO. The signal from fossil fuel CO emissions on the CO₂ concentration field is therefore incorrectly treated as a surface emission of fossil CO₂. Such an overestimation of fossil CO₂ emissions at the surface, mainly over northern hemisphere large fossil fuel emitting regions, leads to an overestimation of the surface CO₂ sink in order to match the interhemispheric CO₂ gradient.

A mathematical formulation of the effect of CO emissions and oxidation on the latitudinal gradient of atmospheric CO₂, and its impact on natural CO₂ fluxes in a 2D inversion ignoring incomplete fuel combustion emitted as CO, which amount to $\approx 0.3 \text{ PgC}$ (latitude-vertical) was given by Enting and Mansbridge (1991). They showed that an inversion that includes an atmospheric CO loop of the carbon cycle placed a larger surface CO₂ sink in the northern tropics and a smaller surface CO₂ sink north of 50°N, compared to an inversion without this process. Using a 3D inversion, Suntharalingam et al. (2005) confirmed the impact of CO oxidation in the atmosphere, although with modest effects on diagnosed land CO₂ fluxes. We describe below an approach to correct for the effect of BVOCs, CO and CH₄ in inversions for RECCAP2. This approach allows the translation of current inversions CO₂ fluxes into total C fluxes that can then be consistently compared with total-C fluxes given by bottom up approaches.

1.4 Correcting net CO₂ ecosystem exchange from inversions for reduced compounds

Separate corrections to inversions should be made for BVOCs, CO and CH₄ because they have very different lifetimes, thus affecting in different ways the CO₂ mole fraction gradients measured by surface networks or satellites. Most BVOCs have a short lifetime and are oxidized to CO₂ in the boundary layer. This means that inversions using CO₂ concentration observations interpret BVOC emissions as local surface CO₂ emissions. Globally, carbon emissions from VOCs amount to 0.8 PgC y^{-1} , mostly biogenic (Guenther et al., 2012) and dominated by isoprene, methanol and terpenes (Folberth et al., 2005). If the purpose



is to compare inversions to Net Ecosystem Exchange (NEE) of total C derived from bottom-up methods (see Section 2) we recommend to include BVOC carbon emissions in bottom-up regional estimates of NEE, rather than making BVOC correction
170 of inversion CO₂ fluxes.

Regarding the effect of the fossil CO loop of the atmospheric CO₂ cycle mentioned above, we propose to treat fossil CO as a ‘bunker fuel’. First, we have to reduce the prescribed prior gridded fossil CO₂ emissions by the gridded amount emitted as CO, using space time distribution of this CO source from inventories or from fossil CO emissions inversion results. Then, we have
175 to prescribe a compensatory prior 3D atmospheric CO₂ source originating from fossil CO oxidized by OH in the atmosphere. Knowledge of thus prior 3D source of CO₂ from fossil origin is now available from atmospheric chemistry models used by global fossil CO emissions inversions since 2000 (Zheng et al. 2019). Other chemistry-transport models simulating the atmospheric oxidation chain of reduced C compounds unconstrained by observations may not be accurate enough for that purpose (Stein et al., 2014). We thus recommend to develop for RECCAP2 new fossil CO₂ emission prior field which include
180 the fossil CO loop. The impact of such new priors will be to reduce inversion estimates of natural CO₂ sinks in the northern hemisphere over regions where fossil fuels are burned, and to enhance sinks in the tropics and subtropics where CO is oxidized into CO₂.

Regarding the effect of CO emissions from wildfires which ranges globally from 0.15 to 0.3 PgC y⁻¹ (Zheng et al., 2019; van
185 der Werf et al., 2017), the action to be taken for inversions depends on the configuration of each system, since inversions do not all use a prior fire emission map, in which case CO from fires could be treated like CO from fossil fuels as explained above. Looking into the three global inversions used in previous global carbon budget assessments, the Jena-Carbo Scope inversion (Rödenbeck et al., 2003) does not have biomass burning a priori CO₂ emissions, the CarbonTracker Europe (CTE) inversion (Peters et al., 2010, Lujikx et al., 2017) prescribes temporal and spatial prior fire emissions which means that any CO₂ uptake
190 by vegetation regrowth after fire will be spread as a diffuse CO₂ sink within and outside burned regions and the CAMS inversion (Chevallier, 2019) prescribes temporal and spatial prior fire emissions and an annual CO₂ uptake equal to annual emissions over each grid cell affected by fires. This setting of CAMS forces an annual regrowth of forests after burning, yet allows the inversion to temporally allocate this regrowth uptake. CTE and CAMS consider that all prior fire emissions are CO₂ emissions, ignoring incomplete combustion emissions of CO. Thus, just as in fossil CO₂ emissions, CTE and CAMS inversions
195 will over-estimate the prior values of CO₂ mixing ratios over burned areas during the fire season. Given the lifetime of CO and given the fact that most biomass burning takes place in the tropics, prescribing all prior fire emissions as CO₂ in CTE and CAMS will cause only a small positive bias in prior CO₂ mixing ratio at tropical stations. The situation may be different for satellite inversions assimilating column CO₂ data. These inversions do sample CO₂ plumes resulting from biomass burning, but not co-emitted CO. In that case, it is expected that inversions based on satellite observations will capture biomass-burning
200 CO₂ emissions, but underestimate fire C emissions by the amount of CO emitted by fires. Carbon emitted as CO by fires will contribute after its oxidation to the global CO₂ growth rate. This signal will thus be wrongly interpreted by inversions as a



diffuse CO₂ source spread uniformly over land and ocean. For RECCAP2, we recommend to pursue research to include CO₂ fluxes from the fire CO-loop as a prior field, to be tested by the inversions which already have fire prior emissions in their settings.

205

Regarding the effect CH₄-carbon emitted over land and oxidized into CO₂ with a lifetime of 9.6 years, thus impacting the interpretation of inversion results, we separate conceptually the effects of fossil versus biogenic CH₄ emissions. Fossil CH₄ fugitive anthropogenic emissions from oil, coal and gas contribute after atmospheric oxidation to the CO₂ growth rate by 0.08 PgC y⁻¹ (Saunois et al., 2020; their top-down estimate) some years after the emission has occurred. This signal is interpreted by inversions as a uniform surface natural CO₂ source over land and ocean. We thus recommend to remove that source uniformly distributed over each grid cell and each month from inversion posterior gridded fluxes to obtain gridded natural land and ocean CO₂ fluxes. A more complex treatment of this fossil CH₄ loop of the atmospheric CO₂ cycle, like proposed above for the fossil CO loop is not a priority in RECCAP2 because of the small magnitude of fossil CH₄-carbon compared to fossil CO one. Biogenic CH₄ emissions from agriculture, inland waters, waste and wetlands amount globally to 0.3 PgC y⁻¹ (Saunois et al., 2020; their top-down estimate) and get oxidized by OH to create a global CO₂ source of the same magnitude. This source will be included in inversions gridded fluxes as a spatially uniform emission over land and ocean. Nevertheless, unlike for fossil CH₄ emissions, this source is compensated by CO₂ sinks from photosynthesis over ecosystems releasing CH₄ (paddy rice areas, grazed lands and wetlands). Inversions will capture the global effect of these CO₂ sinks, but not their spatial patterns, given the low density of the surface network over CH₄ emitting areas. Thus, we will not recommend a correction of gridded inversions CO₂ fluxes for the effect of biogenic CH₄-carbon emissions.

210

215

220

1.5 Adjustment for ‘lateral fluxes’ in CO₂ inversions to compare them with bottom-up C budgets

With the above-recommended treatment of reduced-C emissions, inversions in RECCAP2 will provide gridded and regional means of land atmosphere C fluxes. Inversions form a complete approach, but to compare their regional C fluxes with bottom C stock changes, attention needs to be paid to lateral C fluxes, as done partially by Kondo et al. (2020) and Piao et al. (2018) and comprehensively by Ciais et al. (2020) for RECCAP1 regions. For conversion of C storage change to land-atmosphere C fluxes using lateral fluxes, we recommend to use the same methodology than in Ciais et al. (2020). The section below defines bottom-up C budgets in a way that makes it possible to match them with inversion results.

225

2 Bottom-up carbon budgets

Bottom-up approaches encompass various methods to quantify regional C budgets and their component fluxes. There is no single observation-based bottom-up method giving comprehensively all terrestrial CO₂ or C fluxes. The currently-incomplete scope of existing bottom-up estimates is a source of uncertainty when trying to combine top-down with bottom-up, or when using one of these approaches to verify the results of the other (Kondo et al. 2020; Ciais et al. 2020). For improving the

230



completeness of regional bottom-up C budgets in RECCAP2, we define below a reasonable number of component C fluxes that can all be estimated from observations. In most cases, full observation-based estimates of component C fluxes are not
235 feasible, but limited observations can be generally extrapolated using empirical models to the scale of RECCAP2 regions.

Figure 2 displays the required set of component C fluxes between the land and the atmosphere to be estimated for each region. No unique dataset or method is imposed to estimate each individual C flux, but we give wherever possible references of existing datasets that already quantified those fluxes. Two criteria informed the selection of C fluxes that we recommend for
240 reporting in the RECCAP2 budgets: 1) there exists at least one estimate of each flux available at regional scale that can be used as a default Tier in the case where no regional new estimate can be obtained; 2) each flux is a non-negligible component of the global land C budget, typically an annual flux larger than 0.1 Pg C yr⁻¹ and thus cannot be ignored. If more detailed C fluxes are available for some RECCAP2 regions, we recommend these to be regrouped into the categories shown in Fig. 2, and this grouping to be described.

245

The general recommendation is, where possible, to provide several estimates for each C flux, based on different approaches. This could take the form of ensemble medians and ranges from different models. In the case where one estimate is thought to be more realistic than others, for instance a model with a better score when benchmarked against observations or a higher spatial resolution dataset with better ground validation, the underlying reasons for preferring that estimate need to be explained,
250 based on peer reviewed literature or evaluation. Uncertainty can be calculated from the spread of different estimates, in those cases where the state of knowledge cannot establish that one estimate is better than another. The use of IPCC methods (Mastrandrea et al., 2011) and uncertainty language (http://climate.envsci.rutgers.edu/climdyn2013/IPCC/IPCC_WGI12-IPCCUncertaintyLanguage.pdf) is recommended when different estimates of the same component C flux are available. If different estimates report their own uncertainty, either based on data or an evaluation of the method used, e.g. by performing
255 sensitivity analysis through changing model parameters, input datasets, randomly varying input data, this information should be used to evaluate consistency between estimates, given their uncertainties. It is recommended to use the word ‘uncertainty’ when comparing different estimates and ‘error’ for the difference between an estimate and true values. Because ‘truth’ is unknown for component C fluxes at the scale of large regions, errors cannot be estimated in RECCAP2.

2.1 Net carbon stock change

260 The net carbon stock change of terrestrial ecosystems C pools in a region (ΔC in Fig. 2) can be obtained by repeated inventories of live biomass, litter (including dead biomass), soil carbon and of carbon stock change in wood and crop products. None of the RECCAP2 region has a complete gridded inventory of all carbon stocks and their change over time. Some regions, like North America, China, Europe, Russia have forest biomass inventories established long ago by forest resource agencies (Goodale et al., 2002; Pan et al., 2011). A few countries e.g. England and Wales (Bellamy et al., 2005) and France (Martin et
265 al., 2011) have repeated soil C inventories that allow trends to be quantified. May other countries have single-time soil carbon



inventories (e.g. US, Australia, Germany). Many regions are able to make estimates of carbon stocks in products, from forestry, wood use and crop production statistics.

For RECCAP2, we recommend that each region reports carbon stock changes in all the listed terrestrial ecosystem aggregated
270 pools in Fig. 2, namely ΔC_{forest} , $\Delta C_{croplands}$, $\Delta C_{grasslands}$ and ΔC_{others} , and specify which sub-pools are include in each case. The
sub-pools can include, but are not limited to the following: biomass, litter and woody debris, and soil mineral and organic
carbon. Where attribution of these pools or sub-pools to biomes, land cover types, or political units is made by a regional
synthesis group, the corresponding areas involved must be systematically reported. This includes the definition of the reporting
depth for soil C stocks (0-30 cm and 0-100 cm are recommended). The choice of how many biomes are reported needs to
275 balance data availability with the importance of carbon stock and carbon stock changes within particular biomes (typically a
reported biome should contribute at least 10% of the regional C changes). Regions with significant wetland C or permafrost C
stocks may report this C stock separately, especially in the case where the areas involved occur in different biomes, but this
must be done in a way that allows the C stocks to be subtracted from the biome total, or added back into it, without double
counting. The area of biomes for which no carbon storage or carbon storage change is available needs to be reported and a
280 default value of -9999 should be given to such stocks and their stock change value. The biomes with no data can be specified
(preferable if the area and stock involved is potentially large, since this identifies gaps needing future work), or simply lumped
under ‘others’ if they are minor.

The net C stock change of biological products pools also needs to be reported for crop, wood and other carbon-containing
285 products (see Fig. 2). The depletion of peat C stocks for use as a fuel $\Delta C_{peat\ use}$ in Fig. 2 and thus causing C emissions to the
atmosphere, was significant in the early 20th century in some northern countries, and still is today in few countries (Conchedda
and Tubiello, 2020). It should be reported where relevant, using regional data if available (Joosten, 2009). In the case of C
stock change in wood products ($\Delta C_{wood\ products}$), if possible the change in those wood products in use (e.g., construction, paper)
should be reported separately from those in waste, undergoing decay (e.g. landfills). The names and definitions of the wood
290 product pools considered should be specified. The C stock change of crop product pools ($\Delta C_{crop\ products}$) on an annual time scale
is usually small. It can be reported if data are available, otherwise a value of zero can be assumed. The net carbon stock change
as organic carbon accumulation in lakes and reservoirs, known as burial. (ΔC_{burial}) should be reported based on regional data
or global estimates (Mendonça et al., 2017, Maavara et al., 2017).

2.2 Lateral displacement fluxes within and between regions

295 One of the reasons why net land-atmosphere C exchange excluding fossil fuel emissions, hereafter called Net Ecosystem
Exchange (NEE) of a region is not equal to the net carbon stock change in the same region is because of lateral C fluxes, as
alluded to in Section 1.5. Carbon is lost by each region to the adjacent estuaries through river export; lost or gained through
the trade of crop, wood and animal products; and through the atmospheric transport and deposition of C particles emitted with



300 dust in dry regions. In order to allow the net C stock change estimates to be corrected, we recommend that lateral fluxes in and out of each RECCAP2 region be reported. The main ones are river C export and those from wood and crop trade, as denoted by the red arrows in Fig. 2. A strong point of the RECCAP2 project is an attempt at mass balance closure between pools and fluxes. Therefore, lateral displacement fluxes of C *within* each region, but between pools denoted by the brown arrows in Fig. 2, should also be reported or calculated by mass balance. More details on these fluxes is given below.

2.2.1 Riverine carbon export to estuaries and the coastal ocean

305 Lateral C export fluxes in rivers (F_{rivers} in Fig. 2) should be reported at the interface between rivers and estuaries. We recommend to top the ‘land’ at the mouth of rivers, and to take estuaries being coupled to the coastal ocean by dynamical and biogeochemical processes as ‘blue carbon’ in RECCAP2. Mangroves and salt marshes export large fluxes of dissolved and particulate C produced in upland systems or within riverine systems to estuaries and the coastal ocean (Bauer et al., 2013). These fluxes determine the carbon budget of the aquatic coastal margin ecosystems and we recommend that they should also
310 be considered as ‘blue carbon’. River C fluxes at the river mouth into estuaries can be estimated from dissolved organic carbon (DOC), dissolved inorganic carbon (DIC) and particulate organic carbon (POC) concentration data for the rivers involved, and the associated river flow rates (Ludwig et al., 1998; Mayorga et al., 2010; Dai et al., 2012). Few RECCAP2 regions (Fig. 1) receive C by rivers entering their territory. If this is the case, this input of flux of fluvial carbon from rivers should be reported, even though for simplicity it is not represented in Fig. 2. Evasion from aquatic systems to the atmosphere is treated in Section
315 2.2.7.

2.2.2 Inputs of carbon to riverine from soils and weathered rocks

The inland water carbon cycle receives C leached or eroded from soils as an input. This carbon can be redeposited and buried in the freshwater ecosystems, outgassed to the atmosphere or exported to estuaries and the coastal ocean. This flux is called $F_{bio\ river\ input}$ in Fig. 2. It cannot be measured directly at large spatial scales. We therefore recommend to calculate it by mass
320 balance as the sum of burial, outgassing and export. Similarly, weathering processes consume atmospheric CO₂ (see Section 2.7). This C is subsequently delivered as dissolved bicarbonate ions to rivers. At the global scale and over long timescales, the average proportion of bicarbonate in waters is two-thirds derived from atmospheric C and one third from lithogenic C. We recommend to calculate this weathering-related DIC flux called $F_{litho\ river\ input}$ in Fig. 2, using geological maps and global weathering rates (Hartmann et al., 2009).

325 2.2.3 Carbon fluxes in and out each region due to trade

Net trade related C fluxes for wood and crop products exchanged by each region with others need to be reported in C units, using statistical economic data on trade volume and the carbon content of each product. These are available from regional datasets or using FAOSTAT and GTAP data, or the global dataset of (Peters et al., 2012). This net trade flux should be reported separately for crop products and wood products ($F_{crop\ trade}$ and $F_{wood\ trade}$ in Fig. 2). If relevant it can be reported for animal



330 products as well - but this flux is much smaller than that in crops and wood, and is therefore and is not shown in Fig. 2. Our
best-practice recommendation is to separate the net trade C flux into gross fluxes of imports and exports. The list of
commodities included and ignored should be specified where they are material; commodities making a small contribution can
be lumped under ‘other’.

2.2.4 Crop and wood product transfers within in each region

335 Figure 2 links the C stock change of terrestrial ecosystem pools to the change of C storage in biological wood products by the
harvest and lateral displacement of crop and wood. The harvest of grass for forage can be assumed to be given to animals
locally and can be included in $F_{grazing}$ (see details in Section 2.4). We recommend reporting the total amount of C harvested as
wood and crops in each region as $F_{wood\ harvest}$ and $F_{crop\ harvest}$ (Fig. 2). Subtracting trade fluxes from the harvest fluxes will
provide the C flux displaced within each region for domestic activities. Note that non-harvested and non-burned residues for
340 crops and forests harvesting, such as slash and felling losses should not be part of the harvest flux and should rather be counted
as part of F_{LUC} and $F_{land\ management}$. We note that this locally-decomposing flux is globally large, in 2000 amounting to 1.5 Pg C
 y^{-1} for crop residues and 0.7 Pg C y^{-1} for felling losses in forests (Krausmann et al., 2013).

2.3 Net Ecosystem Exchange

More than a decade ago, there were a number of papers trying to reconcile different definitions of land carbon fluxes (NEE,
345 NEP, NBP, NECB, etc.). Particularly, the papers by Schulze et al. (2000), Randerson et al. (2002), and Chapin et al. (2006).
Schulze et al. focused on the importance to account for disturbance C losses at site scale when considering an ecosystem over
a long time period, hence to separate Net Ecosystem Production (NEP = Gross Primary Productivity minus Ecosystem
Respiration) from Net Biome Production (NBP or Net biome productivity = NEP minus disturbance emissions). Randerson et
al. argued that the net carbon balance should be described by a single name NEP, provided that this flux includes all carbon
350 gains and losses at the spatial scale considered. Last, Chapin et al. in a ‘reconciliation’ paper proposed to use Net Ecosystem
Carbon Balance (NECB) for the net C balance of ecosystems at any given spatial or temporal scale, and to restrict the use of
NEP to the difference between Gross Primary Productivity minus Ecosystem Respiration. Those three definitions consider the
C balance from the point of view of ecosystems. Here we seek to estimate the atmospheric C balance of ecosystems, at the
spatial scale of large regions and the temporal scale of one decade which we call Net Ecosystem Exchange (NEE). NEE is
355 defined as the exchange of all C atoms between a land region and the atmosphere over it, excluding fossil fuels and cement
production emissions. We use a similar definition than Hayes (2012), extended to include natural geological emissions and
sinks, acknowledging that geological fluxes are not from ecosystems per se. NEE includes biogenic atmospheric emissions of
CO, CH₄ and VOCs, all expressed in C units. This definition of NEE matches the land-atmosphere flux of total C that inversions
estimate, provided they account for CO₂, CH₄, CO and VOC fluxes. NEE cannot be derived using the bottom-up approach
360 from a single observation-based approach. Various bottom-up datasets and methods must be combined to obtain each
component flux, then those fluxes can be summed up to NEE.



365

We acknowledge that the geological fluxes are not strictly speaking from ecosystems, and we could therefore have called this flux net terrestrial carbon exchange rather than NEE, but the former terminology could be ambiguous, since some might assume that it includes fossil fuel and cement. NEE also includes biogenic emissions of CO, CH₄ and VOCs, all expressed in C units. This definition of NEE matches the land-atmosphere flux of total C that inversions estimate, provided they account for CO₂, CH₄, CO and VOC fluxes. NEE cannot be derived using the bottom-up approach from a single observation-based approach. Various bottom-up datasets and methods must be combined to obtain each component flux, then those fluxes can be summed up to NEE.

We recommend that when a component C flux of NEE contains meaningful amounts of C emitted as CO, CH₄ and VOC, the type and fraction of reduced carbon compound emitted should be reported. For instance, $F_{grazing}$ emits carbon partly as CH₄, F_{fires} emits CO (and a smaller component of CH₄), VOCs and CH₄, $F_{wood\ products}$ emits CO when burned and CH₄ when the products decay in landfills (see Section 2.5), $F_{rivers\ outgas}$, $F_{lakes\ outgas}$ and $F_{estuaries\ outgas}$ emit CH₄ (see Section 2.6) and $F_{geological\ emissions}$ emitting CH₄ as well as CO₂ (see Section 2.7). The CO₂ and reduced C composition of each flux should be reported separately for clarity, both expressed in C units. This level of detail in the reporting will allow a precise comparison with inversion fluxes (see Section 1).

In Fig. 2, the component fluxes that sum to NEE are subdivided for four sub-systems: terrestrial ecosystems, biological products, inland waters and geological pools (excluding those mined for fossil fuel and cement production). The section below describes the C fluxes components of NEE in each sub-system.

385 2.4 Component fluxes of net ecosystem exchange for terrestrial ecosystems

2.4.1 Net Primary Productivity

Net primary productivity (NPP) is the flux of carbon transformed into biomass tissues after fixation by GPP. NPP can be measured in the field using biometric methods, but this method does not measure non-structural carbohydrates, and NPP-acquired carbon lost to exudates, herbivores, leaf DOC leaching, biogenic VOC emissions, and CH₄ emission by plants (Barba et al., 2019). Field measurements thus estimate the biomass production (BPE = sum of carbon in leaves + wood + roots), which is lower than NPP. Different satellite products provide global maps of NPP for the past decades, but the conversion of GPP to NPP is usually made by an empirical carbon use efficiency model (ratio of GPP to NPP) like the BIOME-BGC model for the GIMMS-NPP (Smith et al., 2015) and for MODIS-NPP (Running et al., 2004) or the BETHY-DLR (Wißkirchen et al., 2013a)



395 global products. Field-estimates of BPE can also be combined with satellite products of GPP to derive NPP (Carvalhais et al.,
2014). Discussing uncertainties of satellite NPP and GPP products is not in the scope of this report, but light-use efficiency
formulations used in many datasets tend to ignore the effect of CO₂ fertilization and of soil moisture deficit, which has
motivated attempts to use data-driven models or hybrid models combining process-based leaf-scale photosynthesis models
with satellite data, e.g. FAPAR, like in the P-MODEL (Stocker et al., 2019) or the BESS model for GPP (Jiang and Ryu,
2016). Those models assimilate satellite observations but include the effects of CO₂, diffuse light, or water stress on
400 photosynthesis.

Additional methods can be used to estimate regional NPP. For crop NPP, aggregated estimates can be obtained from yield
statistics and allometric expansion factors (Wolf et al., 2011), the spatial scale being the one at which yield data can be collected
(e.g. farm, county, province, country). For forest NPP, woody NPP can be obtained from forest inventories, some of the sites
405 having several decades of measurements enabling studies of trends. The recommendation for RECCAP2 is to document as
precisely as possible the definition of NPP in the datasets that will be used for each region, and the ecosystems covered in case
of NPP estimates limited to specific ecosystems. Also make it explicit how NPP datasets were obtained and what their possible
limitations are. We recommend that NPP and not GPP should be reported for each region, given that C from NPP links directly
to biomass and soil C inputs, and to partial appropriation by humans and animals in managed ecosystems, harvested C being
410 further displaced laterally and turned into emissions of C to the atmosphere where it is used.

2.4.2 Carbon emissions from soil heterotrophic respiration R

Soil heterotrophic respiration (SHR) is the C emitted by decomposers in soils and released to the atmosphere. Up to recently,
this flux could not be estimated directly but the availability of point scale measurements from 6000 sites (total soil respiration)
and ≈500 for heterotrophic respiration many peer-reviewed literature in the SRDB 4.0 database (Bond-Lamberty, 2018) allows
415 regional and global up-scaling of this flux for averages over a given period (Hashimoto et al., 2015; Konings et al., 2019;
Warner et al., 2019) or with annual variations (Yao et al. 2020) that can be used for RECCAP2.

2.4.3 Carbon fluxes from land use change and land management

The net land use change flux called F_{LUC} includes C gross fluxes exchanged with the atmosphere from gross deforestation,
legacy and instantaneous soil CO₂ emissions, forest degradation emissions, and sinks from post-abandonment regrowth and
420 afforestation/reforestation activities (Houghton et al., 2012). This flux can be positive or negative depending on the region
considered and the balance of gross fluxes. The net land-use change flux results from changes in NPP, SHR and deforestation
fires over areas affected by land use change in the past. In absence of local NPP and SHR measurements over areas subject to
land use change, F_{LUC} should be treated as a separate flux component of NEE in each region. F_{LUC} is widespread in all
RECCAP2 regions and highly uncertain, and its estimates depend on the approach used. More details on the calculation of
425 F_{LUC} are given in Section 4 since estimates of this flux depend on the method used.



The carbon flux exchanged with the atmosphere from management processes, called $F_{management}$, includes a wide range of forest, crop, and rangeland management practices. It is extremely difficult to separate $F_{management}$ from F_{LUC} as it would require to quantify C fluxes from land use change followed by no management in the new land use in F_{LUC} , and C fluxes from additional management activities on top of land use change. In practice, bookkeeping models of F_{LUC} include management of new land use types in the empirical data they use. For instance, forest to cropland land use emissions are based on empirical observations of soil C changes in croplands from multiple sites, which implicitly include tillage, fertilization, cultivars effects but do not separate each of these practices explicitly in each region, due to lack of data. Likewise, $F_{management}$ is not simulated separately in global studies based on DGVM models, and the effects of management are included in F_{LUC} instead, based on the idealized parameterizations of management practices (Arneth et al., 2017). For croplands, DGVM models include crop harvest preventing the return of residues to soils, and some models represent tillage (Lutz et al., 2019) and changes in fertilization (Olin et al., 2015). To our knowledge, there is no DGVM simulating the effect of irrigation, changes of cultivars and rotations (cover crops), and conservation agriculture on C fluxes. For managed forests, several global models include wood harvest (Arneth et al., 2017; Yue et al., 2018) as a forcing do not have a detailed representation of practices, mainly due to the lack of forcing data, although management is represented in some regions (Luyssaert et al., 2018). For pastures, few models include variable grazing intensity, fertilization and forage cut (Chang et al., 2015). In addition to structural DGVM limitations and lack of representation of management precluding an estimate of $F_{management}$ there is no framework to perform factorial simulations with and without land use change and management that would allow to separate $F_{management}$ and F_{LUC} .

F_{LUC} and $F_{management}$ are accounted for by UNFCCC national communications of C fluxes in the LULUCF sector for managed lands. UNFCCC national communications report land use change emissions in their Common Reporting Format (CRF) communications for different bi-directional land-use transitions. These estimates of F_{LUC} have a different system boundary from those simulated by bookkeeping models (Grassi et al., 2018; Hansis et al., 2015; Houghton and Nassikas, 2017). National communications following the IPCC guidelines (Dong et al., 2006) usually do not consider F_{LUC} from land use that occurred more than 20 years before the reporting period, whereas bookkeeping models and DGVMs consider all land use transitions that occurred since 1700. On the other hand, national communications include F_{LUC} from the expansion or urban areas, which is ignored in bookkeeping models and DGVMs. In national communications, $F_{management}$ as defined here is not separately estimated. Its effect is implicitly included in the LULUCF sector based on empirical emission factors that include management practices in the new land use types, in reports of C fluxes of stable land use types (e.g. cropland remaining croplands). Since 75% of the global land ecosystems are managed (Ellis et al., 2010; Liang et al., 2016), it will be a major challenge in RECCAP2 to account comprehensively for F_{LUC} and $F_{management}$ and even more so to reach a harmonized way for comparing estimates between regions. We thus recommend for each synthesis chapter to describe as precisely as possible the components of F_{LUC} and $F_{management}$ and to explain in which cases they are combined together. Note that the emissions of wood products, crop



460 products and grazing are recommended to report as separate fluxes. If they are provided as part of F_{LUC} and $F_{management}$ they should thus be identified separately.

2.4.4 Carbon emissions from fires

465 This flux called F_{fires} represents the emission of all carbon species to the atmosphere from wildfires, prescribed fires, biomass burning, and biofuel burning including CO_2 , CO , CH_4 and black carbon, separated if possible into crop residues burning and other fires. The burning of crop residues occurs through small-scale fires, which continue to be underestimated by global satellite burned area products. Further, some residues are burned out of the field and those emissions are not measurable with satellites. Burning emissions from crop residues can be calculated from fuel consumption and carbon emission factors. Emissions from other fires can be estimated by ground based/aerial surveys (several countries perform such surveys) or from satellite-based datasets based on burned areas such as GFED (van der Werf et al., 2010) (www.globalfiredata.org), or based on fire radiative power such as GFAS (Di Giuseppe et al., 2018). GFED4.1s is an update of the GFED3 product, with updated burned area and complemented by an active fire detection algorithm that improves detection of small fires (van der Werf et al., 2017). In tropical regions, deforestation causes fires (including peat fires in South-East Asia). It is important here to avoid double accounting by checking in each region if C emissions from deforestation fires were already included in land use change emissions F_{LUC} , and, if this is the case, they must be subtracted from F_{fires} .

2.4.5 Carbon emissions from insects grazing and disturbances

475 This flux called $F_{insects}$ represents C emissions to the atmosphere associated with background grazing and sporadic outbreak of insects. It is a significant C emission in regional budgets, though it is usually ignored, and may be estimated as a fraction of NPP or leaf biomass, if data is available, and provided no double counting, or ignored. Insect outbreaks (Kautz et al., 2017) cause direct and committed emissions to the atmosphere beyond the background grazing of a fraction of biomass, as they partly destroy foliage or cause tree mortality (e.g. bark beetles in Canada, Kurz et al., 2008) that induce legacy emissions that can last for several decades. To our knowledge, only few regions have estimates of insects-disturbances induced C emissions at regional scale, e.g. US (Williams et al., 2016), Canada, and some countries in Europe, and this component flux may not be possible to estimate for each RECCAP2 region, in particular the tropical ones.

2.4.6 Carbon emissions from reduced carbon species

485 This flux called $F_{reduced}$ is the sum of emissions to the atmosphere of reduced C compounds, including biogenic CH_4 , biogenic non-methane biogenic volatile organic compounds (BVOC) and biogenic CO (excluding fires). Carbon emitted as CH_4 by wetlands, termites, rice paddy agriculture sources and removed by soils can be estimated by bottom-up approaches, e.g. synthesized in the global CH_4 budget or from atmospheric CH_4 inversions in the case where those inversions report those flux components separately (Saunio et al., 2020). In the framework proposed here, CH_4 emissions from crop and wood products in landfills are counted $F_{crop\ products}$ and $F_{wood\ products}$ and CH_4 -carbon from animals and manure in $F_{grazing}$. Emissions of carbon



490 from BVOC and CO by the vegetation can be obtained from models used to simulate those fluxes for atmospheric chemistry,
after conversion into units of carbon mass. For instance, the CLM-MEGAN2.1 model (Guenther et al., 2012) estimates
biogenic emissions of CO and of ~150 BVOC compounds with the main contributions being from terpenes, isoprene, methanol,
ethanol, acetaldehyde, acetone, α -pinene, β -pinene, t- β -ocimene, limonene, ethene, and propene.

2.4.7 Carbon emissions from biomass grazed by animals

495 This flux called $F_{grazing}$ represents the C emission that incurs from the consumption of herbage by grazing animals, including
the decomposition of animal products used in the bio-economy, the decomposition of manure and direct animal emissions
from digestion. Only the fraction of manure from animals grazing on grass should be accounted for because C emitted from
manure originating from crop-products given to animals is already included in $F_{crop\ products}$. Grass requirements by animals can
be derived from grass biomass use datasets (Herrero et al., 2013). Grass biomass use per grazing animal head in a region can
500 be calculated based on data of total metabolizable energy (ME) of ruminants in each region. Actual grass intake can be derived
from empirical models or from vegetation models that include management of pasture (Chang et al., 2016). Carbon emitted
from grazed grass biomass includes CH₄ emissions from manure C (excreta) and from enteric fermentation, animal CO₂
respiration from grass intake, and C emissions from the consumption and decay of meat and milk products derived from grass
grazing. The C in milk, animal and manure products can be assumed to decay in one year and to be emitted as C to the
505 atmosphere. Here ‘animals’ are domestic or wild mammals, but not insects.

2.5 Component fluxes of net ecosystem exchange from biological products

2.5.1 Carbon emissions from crop biomass consumed by animals and humans

This flux called $F_{crop\ products}$ represents the carbon emissions to the atmosphere from the consumption of harvested crop
products. It can be calculated from agricultural statistics as the sum of domestically harvested products minus net export minus
510 storage in each region. Crop products are consumed both by animals (including wild animals) and humans, and a distinction
may be made between these two groups of consumers if additional data on consumption type are available in each region. The
digestion of crop products by ruminants emits CH₄-carbon and double counting must be avoided in case this CH₄-C flux is
included in another C flux, like ruminant methane emissions. A fraction of C in consumed crop products is also channeled to
sewage systems and lost to rivers as DOC instead of being emitted to the atmosphere, globally 0.1 PgC yr⁻¹ (Regnier et al.,
515 2013). Although it is a small flux, we recommend to include it in regional budgets if data is available. River CO₂ outgassing
flux estimates should contain the fraction of this sewage C flux returned back to this atmosphere.

2.5.2 Carbon emissions from harvested wood products used by humans

This flux called $F_{wood\ products}$ represents a net carbon emission to the atmosphere from the decay and burning of harvested wood
products used for paper, furniture, and construction. The emission from decay, $F_{wood\ products\ decay}$, can be calculated with models



520 of the fate of wood products in the economy (Eggers, (2002), Mason Earles et al., (2012)) forced by input to products pools
from domestic harvest of non-fuel wood net export of wood products. The small fraction of wood-product waste going to
sewage waters and rivers can also be estimated if relevant data are available. If $F_{wood\ products\ decay}$ is calculated in carbon units,
e.g. from a model of wood product pools, it also includes carbon lost to the atmosphere as CH₄ in landfills, thus double
accounting must be avoided in case CH₄-C emissions from wood in landfills are also reported separately in a region. The flux
525 from burning of wood products, $F_{wood\ product\ burning}$ can be estimated from statistics of fuel wood consumption and carbon
emission factors during combustion (including CO₂, CO and CH₄). This flux should include emissions from commercial
fuelwood burned to produce electricity, and non-commercial fuel wood gathered locally and burned in households, and fuel
wood burned as a fuel by industry. It is important to note that we recommend here to report $F_{wood\ products}$ for each RECCAP2
region as a separate flux. This term is usually included in F_{LUC} in C budget studies based on DGVMs and bookkeeping models
530 (Friedlingstein et al., 2019). It should then be removed from currently reported estimates of F_{LUC} in order to avoid double
counting.

2.6 Component fluxes of net ecosystem exchange for inland waters

2.6.1 Carbon emissions from rivers, lakes and reservoirs

The fluxes called $F_{rivers\ outgas}$ and Flakes +reservoirs outgas in Fig. 2 correspond to those from the outgassing of C from lakes
535 and rivers, respectively. There are two global observation-based estimates of this flux calculated using the same GLORICH
river pCO₂ database, but with different data selection criteria and up-scaling techniques. The one of Raymond et al. (2013)
was produced using the COSCAT regions that represent groups of watersheds, and can be re-interpolated to the RECCAP2
regions. The one of Lauerwald et al. (2015) was produced on a 0.5° × 0.5° global grid and does not include lakes. Gridded
CO₂ emissions of boreal lakes have been estimated separately by Hastie et al. (2018) using an empirical model trained on pCO₂
540 data from mainly Swedish and Canadian lakes. The riverine CO₂ evasion outgassing flux from Lauerwald et al. (2015) is about
half that of Raymond et al., due to lower estimates of average river pCO₂ for the tropics and Siberia resulting from a more
restrictive data selection process and additional averaging effects from the statistical model applied. In addition, the estimates
by Lauerwald et al. (2015) do not account for CO₂ emissions from headwater streams, which may be substantial. For instance,
Horgby et al. (2019) estimated that mountain streams alone emit about 0.15 PgC y⁻¹ globally. Some land models have been
545 developed to include the land to ocean loop of the carbon cycle and their output may be used to assess river and lakes CO₂
evasion fluxes for selected regions (Hastie et al., 2019) or the globe. These models have also confirmed previous observational
findings (e.g. Borges et al., 2015) that river floodplains are a potentially significant, yet overlooked component of the inland
water C budget. Up until now, however, only CO₂ outgassing from rivers, lakes and reservoirs has been considered in regional
C budgets. New synthesis estimates of CH₄ emissions from those inland waters are now available from the CH₄ budget
550 synthesis (Saunois et al., 2019) and we recommend that this source in C units should be added to $F_{rivers\ outgas}$ and $F_{lakes\ +reservoirs\ outgas}$.



2.7 Component fluxes of net ecosystem exchange from geological pools

2.7.1 Geological carbon emissions

This flux called $F_{\text{geological emissions}}$ correspond to natural emissions of CO₂ and CH₄ from geological pools. The Earth's degassing
555 of geological carbon consists of geogenic CO₂ emissions of 0.16 PgC y⁻¹ (Mörner & Etiope, 2002), microbial oxidation of rock
carbon (Hemingway et al., 2018) and CH₄ emission estimated to be 0.027 Pg C y⁻¹ (Etiope et al., 2019) but recently revised
(Hmiel et al., 2020) to a smaller value of 0.0012 Pg C y⁻¹. Geogenic CH₄-C land emissions are from volcanoes, mud volcanoes,
geothermal sources, seeps and micro-seepage, and if the gridded dataset of Etiope et al. (2019) is used, we recommend to
remove the marine coastal seepage CH₄-C emissions reported separately in this dataset. Geogenic CO₂-C emissions are almost
560 exclusively related to geothermal and volcanic areas (high-temperature fluid-rock interactions, crustal magma and mantle
degassing). We suggest here to report these fluxes if there is a published estimate in the region considered.

2.7.2 Weathering uptake of atmospheric CO₂

This flux called $F_{\text{weathering uptake}}$ corresponds to the weathering of carbonate and silicate rocks which is a net sink of atmospheric
CO₂, and corresponds to C then transferred by rivers to the ocean. We recommend that these fluxes should be reported for each
565 region as they are needed to rigorously compare the output of CO₂ inversions (which cover all CO₂ fluxes) with bottom-up
NEE estimates (Fig. 2). This can be achieved using for instance the global dataset from Hartmann et al., (2009) and the gridded
product of Lacroix et al., (2020). Weathering of cement is represented in Fig. 2 and should be reported as part of fossil fuel
emissions, which is not the scope of this paper

3 Methods to estimate bottom up components of NEE

570 The methods described here are:

- C stock changes from ground based estimates (forest biomass and soil carbon inventories)
- CO₂ fluxes measured by Eddy-Covariance
- Other ground-based measurements (e.g. pCO₂ in rivers, site NPP, soil respiration data)
- Models driven by statistical data (e.g. wood and crop products and grazing emissions)
- 575 - Models driven by satellite data (e.g. fire emissions models, NPP models)
- Process-based terrestrial carbon cycle models (e.g. TRENDY models)

The general approach of RECCAP2 is to use more than one of these approaches for each flux, to gain further insights into the
carbon budget of a region by exploring the full range of data available. The purpose of this section is to describe what each
580 method does and does not estimate in terms of NEE component C fluxes as defined in Section 2 and illustrated in Fig. 2, and
therefore what valid comparisons can be made.



3.1 Inventory-based measurements of carbon stock changes

This approach generally uses biomass determined from repeated forest inventories. The stock changes for the LULUCF sector in UNFCCC communications reports are usually based on inventories. In some countries these have been done for many years, but in many countries, they are not available. The sampling density and sampling schemes vary greatly between countries and regions (Pan et al., 2011). The Global Forest Biomass Biodiversity Initiative (<https://www.gfbinitiative.org>) contains 1.2 million forest plots, mainly in the Northern Hemisphere countries, although data are currently not publicly available. The forest inventory data for tropical regions typically comes from research plots, rather than production forests. Forest inventories measure aboveground biomass, from which C stocks can be derived (and stock changes in case of repeated census) but do not quantify soil carbon changes. Repeated inventories of soil carbon only exist in very few countries or regions; where they do, they are often focused on agricultural soils alone. If site history information is available, the repeated inventories of biomass and soil C can be used to F_{LUC} over time, for various land practices.

Point-scale data from inventories can be up-scaled (by simple averaging, or including spatial trends and covariates by using geo-statistics, or more recently by using machine learning) to provide regional budgets of C stock changes in biomass and soils. Forest biomass inventory estimates of tree mortality can further be used to estimate C stock changes for pools which are not directly measured, like litter and soil C, given assumptions regarding their mean residence times. For instance, in their global synthesis of forest C stock changes, Pan et al. (2011) used simple fractions of growing stocks to estimate soil carbon changes. In national inventories, more detailed models of soil C change can be used.

C stock changes are assumed to be the sum of NEE and lateral C fluxes exported from or imported into the territory considered. For RECCAP2, this territory is the area of each region, where the lateral fluxes consist of C exported to the ocean via inland waters, and exported or imported from trade routes, as it is impractical to have observation-based gridded datasets of lateral fluxes at sub-regional resolution. Therefore, when comparing observation-based C-stock change estimates with independent NEE estimates, e.g. from inversions or other sources, it is strongly recommended to first correct the stock change from each region by the net import or export of C in trade and by the export in rivers. In RECCAP2, there is potential to use smaller sub-regions than in RECCAP1, so that some regions may also receive incoming C, in rivers entering their territory.

3.2 Eddy covariance networks

Eddy-covariance flux tower networks measure the net CO₂ flux of terrestrial ecosystems (NPP-SHR) across a global network with a typical footprint of about 1 km². The networks currently consist of about 600 sites (Jung et al., 2020). Given the small footprint, flux tower sites do not adequately measure the fluxes of $F_{geological}$, F_{fires} , $F_{reduced}$, $F_{rivers + lakes outgas}$ (except for a very few towers in wetlands or flooded systems), $F_{crop products}$ and $F_{wood products}$. For $F_{grazing}$, only the fraction emitted as CO₂ by livestock in the field (not in the barn) in the footprint of a tower is measured. Too few towers are installed over ecosystems in



615 transition at different times after a land use change, and the network is potentially biased toward younger, more productive,
forest stands, so that regional estimates of F_{LUC} cannot be directly obtained from eddy-covariance flux towers measurements.
The small spatial footprint of eddy flux towers can be up-scaled into gridded maps of NPP-SHR (NEE at ecosystem level)
using the relationship between the continuous measurements from flux towers and simultaneously recorded climate and
vegetation parameters. The fluxes are up-scaled using gridded predictors from remote sensing (such as FAPAR or NDVI) and
climate fields, using machine learning or data-assimilation techniques (Jung et al., 2020; Tramontana et al., 2016).

620

Both inventories and eddy covariance networks provide point sampling with many gaps between points. These gaps are filled
using up-scaling models like FLUXCOM (Jung et al., 2020; Tramontana et al., 2016). The FLUXCOM data show fair
agreement with inversions and TRENDY models for the seasonal cycle of NEE and for the phase of inter-annual NEE
anomalies (Jung et al., 2017) but the absolute magnitude of interannual anomalies is strongly under-estimated. One attempt to
625 close the global NEE budget by combining FLUXCOM estimates of NPP – SHR with other fluxes not measured by flux towers
(Zscheischler et al., 2015) obtained a net sink of CO_2 larger by 10 PgC y^{-1} than the net land CO_2 sink deduced from the global
budget. One possible reason for this mismatch could be biases introduced during the processing of micro-meteorological
observations, for instance u^* filtering, or the sampling bias in the tower network. The tower sites are not randomly distributed,
and therefore measure fewer recently disturbed ecosystems (typically C sources) than recovering ones (C sinks), thus
630 overestimating CO_2 uptake given the available network. Since we do not know the true distribution of land fluxes, up-scaling
models of flux towers data could miss important ecosystems not sampled by the training data, or representative landscape
elements with intense sources (peatlands, permafrost, disturbed ecosystems) or sinks (peatlands, plantations) that might
contribute significantly to the carbon balance of a region.

635 We recommend that RECCAP-2 teams use eddy covariance estimates of net ecosystem CO_2 fluxes, but since they consist only
of NPP – SHR, these fluxes should add other CO_2 fluxes that are not measured by this approach. This can be done using
aggregated estimates of the non-measured C fluxes in each region, or using gridded estimates. For instance, Zscheischler et al.
(2015) used gridded estimates of F_{fires} , $F_{\text{rivers + lakes outgas}}$, F_{LUC} , $F_{\text{crop products}}$ and $F_{\text{wood products}}$. They did not add F_{reduced} but gridded
monthly estimates of this flux could be included in RECCAP2 based e.g. on Guenther et al. (2012). We should remain cautious,
640 noting that NPP-SHR upscaled from eddy flux towers so far gives unrealistically high global CO_2 sinks.

3.3 Other ground-based measurements

The list provided here is not exhaustive. It includes ‘ecological’ measurements of NPP e.g. (Olson et al., 2001), biometric C
stock changes at site level, e.g. (Campioli et al., 2015; Luysaert et al., 2007), soil respiration e.g. the SRDB database (Bond-
Lamberty and Thomson, 2010) and pCO_2 data in rivers and lakes (GLORICH). These measurements are sparse and local in
645 nature. In a similar fashion to the flux towers measurements described above, it is possible to derive empirical relationships
linking point data with local climate and other predictor variables; these relationships can then be used for spatial or temporal



extrapolation using gridded fields of the same predictors. In recent years, gridded estimates have been provided for soil respiration (Hashimoto et al., 2015) and soil heterotrophic respiration (Konings et al., 2019; Tang et al., 2019), for $F_{river+lakes}$ $ougas$ (Lauerwald et al., 2015; Raymond et al., 2014), which can be used to create regional totals.

650 3.4 Models driven by statistical data

Here we refer to a variety of models that do not use physical measurements at selected locations, but rather statistical data about harvested C, C in product pools, and C traded or consumed. These data are usually sourced from national or international statistical agencies or sector bodies. Examples are the study of Wolf et al., (2015) who estimated crop NPP, $F_{grazing}$ and F_{crop} $products$, Krausmann et al. (2013) who estimated crop NPP from statistical data on yield, Ciais et al. (2007) who estimated F_{crop} $products$ and the corresponding CO₂ uptake by growing crops and horizontal displacement of harvested crop biomass, and Zscheischler et al. (2015) who provided gridded estimates of F_{wood} $products$ albeit ignoring trade.

3.5 Models driven by satellite data

Satellite data are also used in up-scaling forest inventory, eddy covariance and other ground-based measurements, although giving a full list of this category of models is not the purpose of this paper. Here we refer to satellite-driven NPP models (Bloom et al., 2016; Kolby Smith et al., 2015; Running et al., 2004; Tum et al., 2016; Wißkirchen et al., 2013b) based on light use efficiency formulations, or hybrid land carbon-cycle models that explicitly represent photosynthesis (and NPP), driven by directly-assimilated satellite data. Similarly, fire emission models like GFED and GFAS rely on satellite input data like burned area and fire radiative power (FRP) but estimate emissions using fields from models or other datasets (information on the fuel load, the burning completeness, and emission factors for different gaseous species). Remotely-sensed models of above ground biomass, derived from optical sensors, i.e., MODIS (Baccini et al., 2017), lidar from ICESAT-1 GLAS (Saatchi et al. 2011), synthetic aperture radar or SAR (Santoro et al. 2018), and L-band vegetation optical depth (VOD, Liu et al. 2015) have been produced globally and regionally (i.e., for mangroves using X-band radar, Simard et al., 2019). when they are repeated over time allow estimates of biomass stock change, such as those presented by Brandt et al. (2018) over Africa and Fan et al. (2019) over the tropics. These datasets differ not only by methodology and training datasets, but by spatial resolution (300 meter to 25 km), and by temporal resolution (annual, or epoch), and so an ensemble-based approach is preferable for assessing uncertainty. Below-ground carbon stock estimates are more challenging to access, for live root biomass often a scaling assumption is made, but for mineral and organic carbon, estimates are derived from empirical upscaling or inventory approaches or process-based models described in Section 3.6.

3.6 Process-based terrestrial carbon cycle models

Dynamic global vegetation models (DGVM) simulate bottom-up NEE and a number of ecosystem carbon pools and fluxes, and their change over time on a gridded basis worldwide. The grid resolution ranges from 0.5° for global applications e.g. TRENDY (Sitch et al., 2015) or MstMIP (Wei et al. 2014) to fine resolutions (300 m or less) regionally. These models are not



680 tightly driven by observations (unlike those in 3.5); but some observations are used by modelers to calibrate parameters. TRENDY models now are benchmarked following ILAMB (Friedlingstein et al., 2019). Dense observation datasets are not assimilated systematically, although some Carbon Cycle Data Assimilation Systems exist that make use of DGVMs (Kaminski et al., 2013; MacBean et al., 2016) or simpler models like CARDAMOM (Bloom et al., 2016). The advantages of DGVM models for carbon budgeting are that: 1) they provide ensemble of gridded NEE and NEE component estimates as part of TRENDY, 2) these models should in principle conserve mass and simulate consistent C fluxes and C stock changes for all regions. A limitation of DGVMs apart from the fact that they can differ substantially from observations, is that they do not explicitly represent some of the fluxes in Fig 2. F_{fires} is available from 10 out of 16 DGVM models in TRENDY and FIREMIP (Hantson et al., 2020). F_{LUC} from DGVMs includes a foregone sink of CO₂ called the Loss of Additional Sink Capacity (Gasser et al., 2020; Pongratz et al., 2014) which is not included in data-driven methods to quantify this flux (see Section 4). DGVM models partly include $F_{wood\ products}$ and $F_{crop\ products}$ but assume that all harvest is released locally as CO₂ to the atmosphere, ignoring lateral displacement of harvested C within and across regions. DGVM models ignore $F_{reduced}$ and only one or two include $F_{rivers\ +lakes\ outgas}$. Hence, care should be taken when combining DGVM models output with observation-based estimates of C fluxes because of double counting or undercounting. For instance, C outgassing from rivers and lakes derives from C exported by soils, but if this export is not represented in a DGVM, C will be otherwise released as SHR, so that adding to DGVM output an outgassing flux would lead to an erroneous double accounting.

695 In general, for RECCAP2, we recommend to describe exactly what each estimation approach includes or excludes, for each C flux of Fig. 2, in order to minimize the risk of missing some fluxes or double counting others. Mass conservation should be the key underlying principle when combining bottom up C fluxes originating from different approaches.

4 Fluxes from land-use change

700 Fluxes from land-use change and management (abbreviated to F_{LUC} and defined as having a positive sign for net fluxes from the atmosphere to the land C) are defined as changes in C-stocks due to deforestation, forest degradation and afforestation or reforestation, wood harvest, subsequent regrowth of forest following harvest or agriculture abandonment, conversion between croplands and grasslands (also sometimes called pastures, or more generally, rangelands), as well as management practices such as shifting cultivation (land cyclically rotating between forest and agriculture). Where applicable, peat burning and drainage should also be considered, as well as carbon fluxes related to management practices such as fire management, particularly if those practices have changed within the relevant period (for instance, when historically burning ecosystems are subject to fire suppression, or where fire-protected ecosystems become fire-susceptible) (Alvarado et al., 2020; Forkel et al., 2017; Kelley et al., 2019). Where possible, F_{LUC} should be separated into the component fluxes corresponding to the different processes and adding up to the net regional F_{LUC} . Typical components of F_{LUC} , as reported by bookkeeping models, include immediate biomass losses during deforestation, delayed emissions from soil carbon and litter decomposition for all subsequent



710 years, following land use change (legacy emissions), emissions from wood products harvested as a result of deforestation, or
derived from secondary forests, and recovery gains due to secondary forest regrowth or afforestation (Hansis et al., 2015;
Houghton et al., 2012). Previous versions of the Houghton et al., (2012) bookkeeping model (up until 2017) reported emissions
from shifting cultivation as part of F_{LUC} , but this term has been dropped in the most recent version of this model (Houghton
and Nassikas, 2017). Houghton and Nassikas (2017) also provide emissions from forest degradation (i.e. biomass-reducing
715 activities that do not result in the land parcel being reclassified as a non-forest) and subsequent recovery as part of F_{LUC} .

The various methods available to quantify F_{LUC} (Table 1) rely on different input datasets and models with different abilities to
represent land use practices. They further use different terminology and assumptions on which component fluxes to include,
leading to inconsistencies between one another. For RECCAP2, the best data available in each region should be used. However,
720 it is crucial to define clearly the methods and assumptions made, and which F_{LUC} fluxes are included in the corresponding
results. If possible, regional F_{LUC} fluxes estimated by the "best method" should be compared with those estimated by the global
datasets from the most up-to-date GCP-Global Carbon Budget in order to ensure consistency and comparability between
regions. The methods used to estimate F_{LUC} include: (i) Bookkeeping models (BK), (ii) Dynamic Global Vegetation Models
(DGVM), (iii) Remote-sensing based methods, (iv) National inventories as detailed below.

725 **4.1 Bookkeeping models**

Bookkeeping models rely on present-day vegetation and soil C-densities (aggregated or spatially-explicit) and different
response curves (i.e. time courses of change) to estimate changes in C-stocks following a given transition. The two BK models
used in the Global Carbon Budget (GCB) (Friedlingstein et al., 2019) are those from Houghton and Nassikas (2017) and Hansis
et al. (2015), referred to as H&N and BLUE respectively. Both BK models are able to provide F_{LUC} at country-level, but differ
730 in a number of characteristics, such as the input data, the C-densities and response curves used, the spatial resolution and period
covered, as summarized in Table 1. Spatially-explicit BK models such as BLUE can be adapted to run at regional scales with
finer spatial resolution of land-use change, derived from either national inventories or from remote-sensing (RS) based
transitions (e.g. ESA-CCI Land-cover). If very good data on C-densities and, ideally, response curves, is available regionally,
and no superior regionally BK model is available, BLUE can also be adapted to run with that information at country or regional
735 level.

4.2 Dynamic Global Vegetation Models (DGVMs)

DGVMs explicitly simulate the processes controlling photosynthesis, growth, decomposition and mortality of vegetation and
the processes involved in soil-C changes. They also simulate the fluxes resulting from forest clearing, pasture and crop
conversion, abandonment and re-growth and crop harvest, although the implementation varies between models, as do the
740 assumptions about the areas being converted (e.g. gross versus net conversion, see section 4.5), the management practices
included, and the fate of C following transitions. DGVMs in RECCAP2 can be used to estimate F_{LUC} in two ways: (i) the



global simulations from TRENDY for GCB2019 can be analyzed at country or region level; and (ii) any DGVM including the
aforementioned processes can be forced with better or finer data at country or regional level. If a DGVM with an improved
representation of regional processes is available, it is recommended to use it rather than more generic global models. Yet, it is
important for regional models to follow the simulation protocols of TRENDY (Friedlingstein et al., 2019) to facilitate
comparison between regions. In order to estimate F_{LUC} with DGVMs, factorial simulations with and without LUC from the
pre-industrial period until present are generally used. The year 1700 should be used as the reference data for the pre-industrial
state in RECCAP2, in order to be consistent with the TRENDY protocol in depicting legacy fluxes.

There are different ways to estimate F_{LUC} , which partly explain differences between DGVMs and BK models. The DGVM
simulations used to evaluate F_{LUC} under different assumptions are listed in Table 2. Up to now, F_{LUC} from DGVMs has been
estimated from the difference between two simulations, one forced with changing CO_2 , climate and LUC, and another forced
with changing CO_2 and climate but a fixed pre-industrial land-cover map (corresponding to S2-S3 in the TRENDY protocol).
The potential natural vegetation in the simulation with fixed land cover (S2) is affected by CO_2 fertilization and therefore
provides an additional sink that is lost e.g. when deforestation occurs. This foregone sink is Loss of Additional Sink Capacity
(LASC) (Gasser et al., 2020; Pongratz et al., 2014). For consistency with BK models, F_{LUC} estimates with no LASC and for
present-day C-densities should be delivered instead, based on differences between two simulations under time-invariant
present-day environmental conditions of climate, CO_2 , N-deposition and N-fertilization: one with LUC (S5 in the TRENDY
protocol and Fig. 3) and one with fixed pre-industrial (1700) land cover (S6 in the TRENDY protocol). In that case, F_{LUC} can
be estimated as:

$$F_{LUC-S5} = S5 - S6 \quad (1)$$

Because F_{LUC} from both S5 and BK models are forced with present-day C-densities which have on average increased during
the perturbation of the carbon cycle since pre-industrial times, they may overestimate LUC emission fluxes in the first part of
the last Century. Therefore, an additional simulation (S4) can be performed, where models are forced with time-invariant pre-
industrial environmental conditions, and annual time-varying land use 1700-2018. In that case,

$$F_{LUC-S4} = S4 - S0 \quad (2)$$

where S0 is a control simulation with time-invariant pre-industrial (1700) CO_2 , climate, and land use. In this case, F_{LUC} is
calculated based on pre-industrial potential C densities and does not include LASC. For consistency, the natural land sink over
areas not affected by LUC can then be estimated with DGVMs as:

$$S_{LAND} = S3 - S0 + S6 - S5 = S3 - S4 \quad (3)$$

For RECCAP2, we recommend that F_{LUC} from DGVMs is estimated following Eq. 1 (F_{LUC-S5}) so that results can best be
compared with BK results in the recent decades.



4.3 Remote-sensing data related to LUC

Several global remote-sensing products can be useful in estimating F_{LUC} in RECCAP2. They can be applied in various ways:

775 1) Estimate land-cover change in the recent decades to produce regional transition maps at finer spatial-scale and with better accuracy than are currently available. These maps can then be used to force BK or DGVMs, 2) provide finer-resolution and globally consistent maps of vegetation C-densities (for undisturbed locations) that can be used in BK models, 3) directly estimate changes in biomass C-stocks, for instance using optical data (Harris et al., 2012) vegetation-optical depth (Fan et al., 2019) or Lidar data and report these only for deforestation areas (to exclude environmentally-induced fluxes).

780

Examples of already available remote sensing-based datasets than can be used for land-cover and land cover change mapping are the ESA-CCI Land-Cover product, based on five different satellite missions, at 300m spatial resolution and annual time-steps between 1992 and 2018 (Santoro et al., 2017), the Landsat 30m spatial-resolution forest cover change product covering 2000 to 2018 (Hansen et al., 2013) extended to land cover change for forest, short vegetation and bare soil (Song et al., 2018).

785 For vegetation C-densities, the ESA GlobBiomass dataset provides above-ground biomass data for a period centered on the year 2010 at 100 m spatial resolution (Santoro, 2018). Because of its fine spatial resolution, this dataset could in principle, be used to evaluate undisturbed C-densities (Erb et al., 2018; Luyssaert et al., 2012). Other datasets currently under development include the ESA-CCI high-resolution Land-cover, expected to provide a long-term record since 1990s of regional high-resolution land cover maps at 30 m spatial resolution every 5 years in regions of interest, the ESA-CCI Biomass dataset, which
790 will provide above ground biomass data for four epochs of mid 1990s, 2007-2010, 2017/2018 and 2018/2019 at 100 m spatial resolution with a relative error of less than 20%. The NASA Carbon Monitoring System program is also supporting the development of regional to global scale biomass products based on optical reflectance data from MODIS, as well as active lidar-based approaches using ICESAT-1 and now ICESAT-2 GLAS-retrievals, and the Global Ecosystem Dynamics Instrument or GEDI aboard the International Space Station. The lidar approaches require integration with wall-to-wall optical
795 measurements as lidar is a ‘shot’ retrieval with a fairly small footprint size, but with high-accuracy in terms of measurement ability to retrieve canopy height and thus biomass (Dubayah et al., 2020). Satellite-based products have important advantages for estimating contemporary direct emissions from changes in aboveground biomass, such as global coverage, consistency, reliability, and increasingly-higher spatial resolution. However, they cannot estimate legacy soil fluxes from land-use change prior to the satellite era, nor are they able to separate the contribution of environmental changes on FLUC. The comparison of
800 FLUC derived from RS-based methods with DGVMs or BK estimates should therefore be made with care.

4.4 National inventories

National Greenhouse Gas Inventories (NGHGI) report anthropogenic emissions and sinks to the UNFCCC, and are the official numbers used to take stock of the Nationally Determined Contributions (NDCs). NGHGI use different definitions and assumptions than those used by the carbon-cycle research community, as detailed in (Grassi et al., 2018). NGHGI, in their



805 Agriculture Forestry and Land Use (AFOLU) sector, report CO₂ fluxes of land under management, as defined by each country. Such managed land can include areas under nature conservation management. The C balance of established cropland, grassland and forests are reported from national inventories, under the LULUCF sub-sectors, including C fluxes of transitions involving managed lands. A variety of approaches are used by NGHGs, mostly based on general emission factors following IPCC guidelines. Only lands converted within the past 20 years are included under LULUCF fluxes, unlike BK and DGVM models
810 that land use change fluxes since 1700 or 1850. On the other hand, NGHGI include land use change fluxes for transitions that are usually not implemented in BK and DGVM models, such as from peatland converted to agriculture and from land converted to human settlements.

4.5 Land-use change transitions, definitions and assumptions

The land-use change transitions and land-management fields used in the latest version of the GCP-Global Carbon Budget
815 (Friedlingstein et al., 2019) to calculate the net land use change flux called $FLUC_{latest}$, are from the harmonized land-use change data (LUH2v2.1h) dataset (Hurtt et al., 2011), which is based on HYDE3.1 (Klein Goldewijk et al., 2011). These data have the advantage of being globally consistent and covering a long period (850 - present), but have relatively coarse spatial-resolution (0.25×0.25 -degree) and, due to a globally consistent methodology, may not account for regional specificities (Bastos et al., 2018; Li et al., 2018). For each region, the best available information (in terms of spatiotemporal resolution or
820 detail of processes covered) on land-use change should be used. This can be from national statistics, inventories or remote-sensing. In RECCAP2, each regional team will decide the land cover classification scheme that best fits a given region, but it is recommended that the LUH2v2h forest/non-forest distinction be used when classifying rangelands.

5 Concluding remarks

We present a way forward for developing consistent top-down and bottom-up estimates for regional carbon dioxide budgets.
825 The methodology focuses on reconciling the treatment of non-CO₂ emissions from CH₄, CO, and BVOCs and their contribution to CO₂ via atmospheric chemistry, and the treatment of lateral fluxes of carbon. Given the complexity of this task, the approaches toward implementation can be considered using the Tiered approach of the IPCC, whereby higher Tiers use progressively more complex, regionally and locally calibrated sources of information. For example, a Tier 1 approach combines global emission-factors with activity data to estimate fluxes, Tier 2 might use regionally-calibrated emission factors,
830 whereas Tier 3 uses locally calibrated emission factors to estimate fluxes from activity information. The Global Carbon Project now conducts greenhouse gas budget accounting for the three major greenhouse gases, carbon dioxide, methane, and nitrous oxide, where each budget provides detailed sectoral information for sources and sinks using what is more closely aligned with Tier 1 approaches. Beginning with Tier 1 data can help initiate regional budgets, and identify areas of uncertainty or opportunities for regionally and locally calibrated approaches to be used to reduce uncertainty.



835 **Code and data availability**

There is no code associated to this paper. RECCAP-2 data will be available to the community after submission of each regional chapter to a peer reviewed journal.

Author contributions

840 P.Ciais designed and wrote the study. F. Chevallier provided input to the inversion section and A. Bastos and J. Pongratz contributed the land use section. Other contributors helped to improve the text in their field of expertise or globally. H. Yang additionally helped with the references.

Acknowledgements

P.Ciais acknowledges funding from the ANR CLAND Convergence Institute. A.Bastos, F. Chevallier and P. Ciais acknowledge support from the VERIFY H2020 project and the RECCAP2 ESA CCI project



845 References

- Alvarado, S. T., Andela, N., Silva, T. S. F., and Archibald, S.: Thresholds of fire response to moisture and fuel load differ between tropical savannas and grasslands across continents, *Glob. Ecol. Biogeogr.*, 29(2), 331–344, doi:10.1111/geb.13034, 2020.
- 850 Arneth, A., Sitch, S., Pongratz, J., Stocker, B. D., Ciais, P., Poulter, B., Bayer, A. D., Bondeau, A., Calle, L., Chini, L. P., Gasser, T., Fader, M., Friedlingstein, P., Kato, E., Li, W., Lindeskog, M., Nabel, J. E. M. S., Pugh, T. A. M., Robertson, E., Viovy, N., Yue, C., and Zaehle, S.: Historical carbon dioxide emissions caused by land-use changes are possibly larger than assumed, *Nat. Geosci.*, 10(2), 79–84, doi:10.1038/ngeo2882, 2017.
- Aulagnier, C., Rayner, P., Ciais, P., Vautard, R., Rivier, L., and Ramonet, M.: Is the recent build-up of atmospheric CO₂ over Europe reproduced by models. Part 2: An overview with the atmospheric mesoscale transport model CHIMERE, 855 *Tellus, Ser. B Chem. Phys. Meteorol.*, 62(1), 14–25, doi:10.1111/j.1600-0889.2009.00443.x, 2010.
- Baccini, A., Walker, W., Carvalho, L., Farina, M., Sulla-Menashe, D., and Houghton, R. A.: Tropical forests are a net carbon source based on aboveground measurements of gain and loss, *Science*, 358(6360), 230–234, doi:10.1126/science.aam5962, 2017.
- 860 Barba, J., Bradford, M. A., Brewer, P. E., Bruhn, D., Covey, K., van Haren, J., Megonigal, J. P., Mikkelsen, T. N., Pangala, S. R., Pihlatie, M., Poulter, B., Rivas-Ubach, A., Schadt, C. W., Terazawa, K., Warner, D. L., Zhang, Z., and Vargas, R.: Methane emissions from tree stems: a new frontier in the global carbon cycle, *New Phytol.*, 222(1), 18–28, doi:10.1111/nph.15582, 2019.
- Bastos, A., Peregón, A., Gani, É. A., Khudyaev, S., Yue, C., Li, W., Gouveia, C. M., and Ciais, P.: Influence of high-latitude warming and land-use changes in the early 20th century northern Eurasian CO₂ sink, *Environ. Res. Lett.*, 13(6), 865 doi:10.1088/1748-9326/aac4d3, 2018.
- Bauer, J. E., Cai, W.-J., Raymond, P. a, Bianchi, T. S., Hopkinson, C. S., and Regnier, P. a G.: The changing carbon cycle of the coastal ocean., *Nature*, 504(7478), 61–70, doi:10.1038/nature12857, 2013.
- Bellamy, P. H., Loveland, P. J., Bradley, R. I., Lark, R. M., and Kirk, G. J. D.: Carbon losses from all soils across England and Wales 1978–2003, *Nature*, 437(7056), 245–248, doi:10.1038/nature04038, 2005.
- 870 Bloom, A. A., Exbrayat, J.-F., van der Velde, I. R., Feng, L., and Williams, M.: The decadal state of the terrestrial carbon cycle: Global retrievals of terrestrial carbon allocation, pools, and residence times, *Proc. Natl. Acad. Sci.*, 113(5), 1285–1290, doi:10.1073/pnas.1515160113, 2016.
- Bond-Lamberty, B. and Thomson, A.: A global database of soil respiration data, *Biogeosciences*, 7(6), 1915–1926, doi:10.5194/bg-7-1915-2010, 2010.



- 875 Bond-Lamberty, B.: New Techniques and Data for Understanding the Global Soil Respiration Flux, *Earth's Futur.*, 6(9), 1176–1180, doi:10.1029/2018EF000866, 2018.
- Brandt, M., Wigneron, J., Chave, J., Tagesson, T., Penuelas, J., Ciais, P., Rasmussen, K., Tian, F., Mbow, C., Al-yaari, A., Rodriguez-fernandez, N., Schurgers, G., Zhang, W., Chang, J., Kerr, Y., Verger, A., Tucker, C., Mialon, A., Rasmussen, L. V., and Fan, L.: Satellite passive microwaves reveal recent climate-induced carbon losses in African
880 drylands, *Nat. Ecol. Evol.*, doi:10.1038/s41559-018-0530-6, 2018.
- Campoli, M., Vicca, S., Luysaert, S., Bilcke, J., Ceschia, E., Chapin, F. S., Ciais, P., Fernández-Martínez, M., Malhi, Y., Obersteiner, M., Olefeldt, D., Papale, D., Piao, S. L., Peñuelas, J., Sullivan, P. F., Wang, X., Zenone, T., and Janssens, I. A.: Biomass production efficiency controlled by management in temperate and boreal ecosystems, *Nat. Geosci.*, 8(11), 843–846, doi:10.1038/ngeo2553, 2015.
- 885 Canadell, J., Ciais, P., Sabine, C., and Joos, F.: REgional Carbon Cycle Assessment and Processes (RECCAP). *Biogeosciences*, 9–12, 2015.
- Carvalhais, N., Forkel, M., Khomik, M., Bellarby, J., Jung, M., Migliavacca, M., Mu, M., Saatchi, S., Santoro, M., Thurner, M., Weber, U., Ahrens, B., Beer, C., Cescatti, A., Randerson, J. T., and Reichstein, M.: Global covariation of carbon turnover times with climate in terrestrial ecosystems, *Nature*, 514(7521), 213–217, doi:10.1038/nature13731, 2014.
- 890 Chang, J., Ciais, P., Herrero, M., Havlik, P., Campoli, M., Zhang, X., Bai, Y., Viovy, N., Joiner, J., Wang, X., Peng, S., Yue, C., Piao, S., Wang, T., Hauglustaine, D. A., Soussana, J. F., Peregon, A., Kosykh, N., and Mironycheva-Tokareva, N.: Combining livestock production information in a process-based vegetation model to reconstruct the history of grassland management, *Biogeosciences*, 13(12), 3757–3776, doi:10.5194/bg-13-3757-2016, 2016.
- Chang, J., Viovy, N., Vuichard, N., Ciais, P., Campoli, M., Klumpp, K., Martin, R., Leip, A., and Soussana, J. F.: Modeled
895 changes in potential grassland productivity and in grass-fed ruminant livestock density in Europe over 1961–2010, *PLoS One*, 10(5), 1–30, doi:10.1371/journal.pone.0127554, 2015.
- Chapin, F. S., Woodwell, G. M., Randerson, J. T., Rastetter, E. B., Lovett, G. M., Baldocchi, D. D., et al. Reconciling Carbon-cycle Concepts, Terminology, and Methods. *Ecosystems*, 9(7), 2006.
- Chevallier, F.: Description of the CO₂ inversion production chain. CAMS deliverable CAMS73_2018SC1_D73.5.2.1-
900 2019_201904_CO₂ inversion production chain_v1. Retrieved from <http://atmosphere.copernicus.eu/>, 2019.
- Choulga, M., Janssens-maenhout, G., Super, I., Agusti-panareda, A., Bousseret, N., Crippa, M., Gon, H. D. Van Der, Engelen, R., Kuenen, J., McNorton, J., Oreggioni, G., and Solazzo, E.: Earth system modelling and data assimilation, *Earth Syst. Sci. Data*, (April), 1–37, doi:10.5281/zenodo.3712339.35, 2020.
- Ciais, P., Bousquet, P., Freibauer, A., and Naegler, T.: Horizontal displacement of carbon associated with agriculture and its



- 905 impacts on atmospheric CO₂, *Global Biogeochem. Cycles*, 21(2), 1–12, doi:10.1029/2006GB002741, 2007.
- Ciais, P., Yao, Y., Gasser, T., Baccini, A., Wang, Y., Lauerwald, R., Peng, S., Bastos, A., Li, W., Raymond, P. A., Canadell, J. G., Peters, G. P., Andres, R. J., Chang, J., Yue, C., Dolman, A. J., Haverd, V., Hartmann, J., Laruelle, G., Konings, A. G., King, A. W., Liu, Y., Luysaert, S., Maignan, F., Patra, P. K., Peregon, A., Regnier, P., Pongratz, J., Poulter, B., Shvidenko, A., Valentini, R., Wang, R., Broquet, G., Yin, Y., Zscheischler, J., Guenet, B., Goll, D. S., Ballantyne, A.-
910 P., Yang, H., Qiu, C., and Zhu, D.: Empirical estimates of regional carbon budgets imply reduced global soil heterotrophic respiration. *Natl. Sci. Rev.*, 2020.
- Conchedda, G. and Tubiello, F. N.: Drainage of Organic Soils and GHG Emissions, 1990 – 2019, (July), doi:10.5194/essd-2020-202, 2020.
- Dai, M., Yin, Z., Meng, F., Liu, Q., and Cai, W. J.: Spatial distribution of riverine DOC inputs to the ocean: An updated global
915 synthesis, *Curr. Opin. Environ. Sustain.*, 4(2), 170–178, doi:10.1016/j.cosust.2012.03.003, 2012.
- Dong, H., Mangino, J., McAllister, T. A., Hatfield, J. L., Johnson, D. E., Lassey, K., Aparecida de Lima, M., and Romanovskaya, D.: Intergovernmental Panel on Climate Change (IPCC) Guidelines for National Greenhouse Gas Inventories, Volume 4: Agriculture, Forestry and Other Land Use, Chapter 10: Emissions from Livestock and Manure Management. Kanagawa, Japan, 1-87, 2006.
- 920 Dubayah, R., Blair, J. B., Goetz, S., Fatoyinbo, L., Hansen, M., Healey, S., Hofton, M., Hurtt, G., Kellner, J., Luthcke, S., Armston, J., Tang, H., Duncanson, L., Hancock, S., Jantz, P., Marselis, S., Patterson, P. L., Qi, W., and Silva, C.: The Global Ecosystem Dynamics Investigation: High-resolution laser ranging of the Earth’s forests and topography, *Sci. Remote Sens.*, 1(January), 100002, doi:10.1016/j.srs.2020.100002, 2020.
- Eggers, T.: The impacts of manufacturing and utilisation of wood products on the European carbon budget, 2002.
- 925 Ellis, E. C., Goldewijk, K. K., Siebert, S., Lightman, D., and Ramankutty, N.: Anthropogenic transformation of the biomes, 1700 to 2000, *Glob. Ecol. Biogeogr.*, 19(5), 589–606, doi:10.1111/j.1466-8238.2010.00540.x, 2010.
- Enting, I. G. and Mansbridge, J. V.: Latitudinal distribution of sources and sinks of CO₂-Results of an inversion study. *TellB*, 43, 156-170, 1991.
- Erb, K. H., Kastner, T., Plutzer, C., Bais, A. L. S., Carvalhais, N., Fetzel, T., Gingrich, S., Haberl, H., Lauk, C., Niedertscheider, M., Pongratz, J., Thurner, M., and Luysaert, S.: Unexpectedly large impact of forest management and grazing on global
930 vegetation biomass, *Nature*, 553(7686), 73–76, doi:10.1038/nature25138, 2018.
- Etioppe, G., Ciotoli, G., Schwietzke, S., and Schoell, M.: Gridded maps of geological methane emissions and their isotopic signature, *Earth Syst. Sci. Data*, 11(1), 1–22, doi:10.5194/essd-11-1-2019, 2019.
- Fan, L., Wigneron, J.-P., Ciais, P., Chave, J., Brandt, M., Fensholt, R., Saatchi, S. S., Bastos, A., Al-Yaari, A., Hufkens, K.,



- 935 Qin, Y., Xiao, X., Chen, C., Myneni, R. B., Fernandez-Moran, R., Mialon, A., Rodriguez-Fernandez, N. J., Kerr, Y., Tian, F., and Peñuelas, J.: Satellite-observed pantropical carbon dynamics, *Nat. Plants*, doi:10.1038/s41477-019-0478-9, 2019.
- Folberth, G. A., Hauglustaine, D. A., Ciais, P., and Lathière, J.: On the role of atmospheric chemistry in the global CO₂ budget, *Geophys. Res. Lett.*, 32(8), 1–4, doi:10.1029/2004GL021812, 2005.
- 940 Forkel, M., Dorigo, W., Lasslop, G., Teubner, I., Chuvieco, E., and Thonicke, K.: A data-driven approach to identify controls on global fire activity from satellite and climate observations (SOFIA V1), *Geosci. Model Dev.*, 10(12), 4443–4476, doi:10.5194/gmd-10-4443-2017, 2017.
- Friedl, M. A., McIver, D. K., Hodges, J. C. F., Zhang, X. Y., Muchoney, D., Strahler, A. H., Woodcock, C. E., Gopal, S., Schneider, A., Cooper, A., Baccini, A., Gao, F., and Schaaf, C.: Global land cover mapping from MODIS: Algorithms and early results, *Remote Sens. Environ.*, 83(1–2), 287–302, doi:10.1016/S0034-4257(02)00078-0, 2002.
- 945 Friedlingstein, P., Jones, M. W., O’Sullivan, M., Andrew, R. M., Hauck, J., Peters, G. P., Peters, W., Pongratz, J., Sitch, S., Le Quéré, C., Bakker, D. C. E., Canadell, J. G., Ciais, P., Jackson, R. B., Anthoni, P., Barbero, L., Bastos, A., Bastrikov, V., Becker, M., Bopp, L., Buitenhuis, E., Chandra, N., Chevallier, F., Chini, L. P., Currie, K. I., Feely, R. A., Gehlen, M., Gilfillan, D., Gkritzalis, T., Goll, D. S., Gruber, N., Gutekunst, S., Harris, I., Haverd, V., Houghton, R. A., Hurtt, G., Ilyina, T., Jain, A. K., Joetzier, E., Kaplan, J. O., Kato, E., Klein Goldewijk, K., Korsbakken, J. I., Landschützer, P., 950 Lauvset, S. K., Lefèvre, N., Lenton, A., Lienert, S., Lombardozzi, D., Marland, G., McGuire, P. C., Melton, J. R., Metzl, N., Munro, D. R., Nabel, J. E. M. S., Nakaoka, S.-I., Neill, C., Omar, A. M., Ono, T., Pregon, A., Pierrot, D., Poulter, B., Rehder, G., Resplandy, L., Robertson, E., Rödenbeck, C., Séférian, R., Schwinger, J., Smith, N., Tans, P. P., Tian, H., Tilbrook, B., Tubiello, F. N., van der Werf, G. R., Wiltshire, A. J., and Zaehle, S.: Global Carbon Budget 2019, *Earth Syst. Sci. Data*, 11(4), 1783–1838, doi:10.5194/essd-11-1783-2019, 2019.
- Gasser, T., Crepin, L., Quilcaille, Y., Houghton, R., Ciais, P., and Obersteiner, M.: Historical CO₂ emissions from land-use and land-cover change and their uncertainty, *Biogeosciences Discuss.*, (February), 1–43, doi:10.5194/bg-2020-33, 2020.
- Di Giuseppe, F., Rémy, S., Pappenberger, F., and Wetterhall, F.: Using the Fire Weather Index (FWI) to improve the estimation of fire emissions from fire radiative power (FRP) observations, *Atmos. Chem. Phys.*, 18(8), 5359–5370, 960 doi:10.5194/acp-18-5359-2018, 2018.
- Goodale, C. L., Apps, M. J., Birdsey, R. A., Field, C. B., Heath, L. S., Houghton, R. A., Jenkins, J. C., Kohlmaier, G. H., Kurz, W., Liu, S., Nabuurs, G. J., Nilsson, S., and Shvidenko, A. Z.: Forest carbon sinks in the Northern Hemisphere, *Ecol. Appl.*, 12(3), 891–899, doi:10.1890/1051-0761(2002)012[0891:FCSITN]2.0.CO;2, 2002.
- Grassi, G., House, J., Kurz, W. A., Cescatti, A., Houghton, R. A., Peters, G. P., Sanz, M. J., Viñas, R. A., Alkama, R., Arneeth, 965 A., Bondeau, A., Dentener, F., Fader, M., Federici, S., Friedlingstein, P., Jain, A. K., Kato, E., Koven, C. D., Lee, D.,



- Nabel, J. E. M. S., Nassikas, A. A., Perugini, L., Rossi, S., Sitch, S., and Viovy, N.: Reconciling global-model estimates and country reporting of anthropogenic forest CO₂ sinks, *Nat. Clim. Chang.*, 8(October), doi:10.1038/s41558-018-0283-x, 2018.
- 970 Guenther, A. B., Jiang, X., Heald, C. L., Sakulyanontvittaya, T., Duhl, T., Emmons, L. K., and Wang, X.: The model of emissions of gases and aerosols from nature version 2.1 (MEGAN2.1): An extended and updated framework for modeling biogenic emissions, *Geosci. Model Dev.*, 5(6), 1471–1492, doi:10.5194/gmd-5-1471-2012, 2012.
- Hansen, M. C., Potapov, P. V., Moore, R., Hancher, M., Turubanova, S. A., and Tyukavina, A.: High-Resolution Global Maps of 21st-Century Forest Cover Change, *Science*, 134, 850–854, 2013.
- 975 Hansis, E., Davis, S. J., and Pongratz, J.: Relevance of methodological choices for accounting of land use change carbon fluxes, *Global Biogeochem. Cycles*, 29(8), 1230–1246, doi:10.1002/2014GB004997, 2015.
- Hantson, S., Kelley, D., Arneeth, A., Harrison, S., Archibald, S., Bachelet, D., Forrest, M., Hickler, T., Lasslop, G., Li, F., Mangeon, S., Melton, J., Nieradzick, L., Rabin, S., Prentice, I. C., Sheehan, T., Sitch, S., Teckentrup, L., Voulgarakis, A., and Yue, C.: Quantitative assessment of fire and vegetation properties in historical simulations with fire-enabled vegetation models from the Fire Model Intercomparison Project, *Geosci. Model Dev. Discuss.*, (June), 1–25, doi:10.5194/gmd-2019-261, 2020.
- 980 Harris, N. L., Brown, S., Hagen, S. C., Saatchi, S. S., Petrova, S., Salas, W., Hansen, M. C., Potapov, P. V., and Lotsch, A.: Baseline map of carbon emissions from deforestation in tropical regions, *Science* (80-.), 336(6088), 1573–1576, doi:10.1126/science.1217962, 2012.
- Hartmann, J., Jansen, N., Dürr, H. H., Kempe, S., and Köhler, P.: Global CO₂-consumption by chemical weathering: What is the contribution of highly active weathering regions?, *Glob. Planet. Change*, 69(4), 185–194, doi:10.1016/j.gloplacha.2009.07.007, 2009.
- 985 Hashimoto, S., Carvalhais, N., Ito, A., Migliavacca, M., Nishina, K., and Reichstein, M.: Global spatiotemporal distribution of soil respiration modeled using a global database, *Biogeosciences*, 12(13), 4121–4132, doi:10.5194/bg-12-4121-2015, 2015.
- 990 Hastie, A., Lauerwald, R., Weyhenmeyer, G., Sobek, S., Verpoorter, C., and Regnier, P.: CO₂ evasion from boreal lakes: Revised estimate, drivers of spatial variability, and future projections, *Glob. Chang. Biol.*, 24(2), 711–728, doi:10.1111/gcb.13902, 2018.
- 995 Hastie, A., Lauerwald, R., Ciais, P., and Regnier, P.: Aquatic carbon fluxes dampen the overall variation of net ecosystem productivity in the Amazon basin: An analysis of the interannual variability in the boundless carbon cycle, *Glob. Chang. Biol.*, 25(6), 2094–2111, doi:10.1111/gcb.14620, 2019.



- Hayes, D. and Turner, D.: The need for “Apples-to-Apples” comparisons of carbon dioxide source and sink estimates. *Eos*, 93(41), 404-405, 2012.
- Hemingway, J. D., Hilton, R. G., Hovius, N., Eglinton, T. I., Haghipour, N., Wacker, L., Chen, M. C., and Galy, V. V.: Microbial oxidation of lithospheric organic carbon in rapidly eroding tropical mountain soils, *Science* (80-.), 360(6385), 209–212, doi:10.1126/science.aao6463, 2018.
- Herrero, M., Havlík, P., Valin, H., Notenbaert, A., Rufino, M. C., Thornton, P. K., Blümmel, M., Weiss, F., Grace, D., and Obersteiner, M.: Biomass use, production, feed efficiencies, and greenhouse gas emissions from global livestock systems, *Proc. Natl. Acad. Sci. U. S. A.*, 110(52), 20888–20893, doi:10.1073/pnas.1308149110, 2013.
- Hmiel, B., Petrenko, V. V., Dyonisius, M. N., Buizert, C., Smith, A. M., Place, P. F., Harth, C., Beaudette, R., Hua, Q., Yang, B., Vimont, I., Michel, S. E., Severinghaus, J. P., Etheridge, D., Bromley, T., Schmitt, J., Faïn, X., Weiss, R. F., and Dlugokencky, E.: Preindustrial ¹⁴CH₄ indicates greater anthropogenic fossil CH₄ emissions, *Nature*, 578(7795), 409–412, doi:10.1038/s41586-020-1991-8, 2020.
- Horgby, Å., Segatto, P. L., Bertuzzo, E., Lauerwald, R., Lehner, B., Ulseth, A. J., Vennemann, T. W., and Battin, T. J.: Unexpected large evasion fluxes of carbon dioxide from turbulent streams draining the world’s mountains, *Nat. Commun.*, 10(1), doi:10.1038/s41467-019-12905-z, 2019.
- Houghton, R. A. and Nassikas, A. A.: Global and regional fluxes of carbon from land use and land cover change 1850–2015, *Global Biogeochem. Cycles*, 31(3), 456–472, doi:10.1002/2016GB005546, 2017.
- Houghton, R. A., House, J. I., Pongratz, J., van der Werf, G. R., DeFries, R. S., Hansen, M. C., Le Quéré, C., and Ramankutty, N.: Carbon emissions from land use and land-cover change, *Biogeosciences*, 9(12), 5125–5142, doi:10.5194/bg-9-5125-2012, 2012.
- Hubau, W., Lewis, S. L., Phillips, O. L., Affum-Baffoe, K., Beeckman, H., Cuni-Sanchez, A., et al. : Asynchronous carbon sink saturation in African and Amazonian tropical forests. *Nature*, 579(7797), 80–87. <https://doi.org/10.1038/s41586-020-2035-0>, 2020.
- Hurt, G. C., Chini, L. P., Frohling, S., Betts, R. A., Feddema, J., Fischer, G., Fisk, J. P., Hibbard, K., Houghton, R. A., Janetos, A., Jones, C. D., Kindermann, G., Kinoshita, T., Klein Goldewijk, K., Riahi, K., Shevliakova, E., Smith, S., Stehfest, E., Thomson, A., Thornton, P., van Vuuren, D. P., and Wang, Y. P.: Harmonization of land-use scenarios for the period 1500–2100: 600 years of global gridded annual land-use transitions, wood harvest, and resulting secondary lands, *Clim. Change*, 109(1–2), 117–161, doi:10.1007/s10584-011-0153-2, 2011.
- Jiang, C. and Ryu, Y.: Multi-scale evaluation of global gross primary productivity and evapotranspiration products derived from Breathing Earth System Simulator (BESS), *Remote Sens. Environ.*, 186, 528–547, doi:10.1016/j.rse.2016.08.030, 2016.



- Jones, M., Andrew, R. M., Peters, G. P., Janssens-Maenhout, G., De-Goll, A. J., Ciais, P., et al.: Gridded fossil CO₂ emissions and related O₂ combustion consistent with national inventories 1959-2018. *Scientific Data*, Submitted.
- Joosten, H.: The Global Peatland CO₂ Picture Peatland status and emissions in all countries of the world, 2009.
- 1030 Jung, M., Reichstein, M., Schwalm, C. R., Huntingford, C., Sitch, S., Ahlström, A., Arneth, A., Camps-Valls, G., Ciais, P., Friedlingstein, P., Gans, F., Ichii, K., Jain, A. K., Kato, E., Papale, D., Poulter, B., Raduly, B., Rödenbeck, C., Tramontana, G., Viovy, N., Wang, Y. P., Weber, U., Zaehle, S., and Zeng, N.: Compensatory water effects link yearly global land CO₂ sink changes to temperature, *Nature*, 541(7638), 516–520, doi:10.1038/nature20780, 2017.
- 1035 Jung, M., Schwalm, C., Migliavacca, M., Walther, S., Camps-Valls, G., Koirala, S., Anthoni, P., Besnard, S., Bodesheim, P., Carvalhais, N., Chevallier, F., Gans, F., S Goll, D., Haverd, V., Köhler, P., Ichii, K., K Jain, A., Liu, J., Lombardozzi, D., E M S Nabel, J., A Nelson, J., O’Sullivan, M., Pallandt, M., Papale, D., Peters, W., Pongratz, J., Rödenbeck, C., Sitch, S., Tramontana, G., Walker, A., Weber, U., and Reichstein, M.: Scaling carbon fluxes from eddy covariance sites to globe: Synthesis and evaluation of the FLUXCOM approach, *Biogeosciences*, 17(5), 1343–1365, doi:10.5194/bg-17-1343-2020, 2020.
- 1040 Kaminski, T., Knorr, W., Schürmann, G., Scholze, M., Rayner, P. J., Zaehle, S., Blessing, S., Dorigo, W., Gayler, V., Giering, R., Gobron, N., Grant, J. P., Heimann, M., Hooker-Stroud, A., Houweling, S., Kato, T., Kattge, J., Kelley, D., Kemp, S., Koffi, E. N., Köstler, C., Mathieu, P. P., Pinty, B., Reick, C. H., Rödenbeck, C., Schnur, R., Scipal, K., Sebald, C., Stacke, T., Van Scheltinga, A. T., Vossbeck, M., Widmann, H., and Ziehn, T.: The BETHY/JSBACH Carbon Cycle Data Assimilation System: Experiences and challenges, *J. Geophys. Res. Biogeosciences*, 118(4), 1414–1426, doi:10.1002/jgrg.20118, 2013.
- 1045 Kautz, M., Meddens, A. J. H., Hall, R. J., and Arneth, A.: Biotic disturbances in Northern Hemisphere forests – a synthesis of recent data, uncertainties and implications for forest monitoring and modelling, *Glob. Ecol. Biogeogr.*, 26(5), 533–552, doi:10.1111/geb.12558, 2017.
- Kelley, D. I., Bistinas, I., Whitley, R., Burton, C., Marthews, T. R., and Dong, N.: How contemporary bioclimatic and human controls change global fire regimes, *Nat. Clim. Chang.*, 9(9), 690–696, doi:10.1038/s41558-019-0540-7, 2019.
- 1050 Klein Goldewijk, K., Beusen, A., Van Dreht, G., and De Vos, M.: The HYDE 3.1 spatially explicit database of human-induced global land-use change over the past 12,000 years, *Glob. Ecol. Biogeogr.*, 20(1), 73–86, doi:10.1111/j.1466-8238.2010.00587.x, 2011.
- Kolby-Smith, W., Reed, S. C., Cleveland, C. C., Ballantyne, A. P., Anderegg, W. R. L., Wieder, W. R., Liu, Y. Y., and Running, S. W.: Large divergence of satellite and Earth system model estimates of global terrestrial CO₂ fertilization, *Nat. Clim. Chang.*, 6(3), 306–310, doi:10.1038/nclimate2879, 2016.
- 1055 Kondo, M., Patra, P. K., Sitch, S., Friedlingstein, P., Poulter, B., Chevallier, F., Ciais, P., Canadell, J. G., Bastos, A., Lauerwald,



- 1060 R., Calle, L., Ichii, K., Anthoni, P., Arneth, A., Haverd, V., Jain, A. K., Kato, E., Kautz, M., Law, R. M., Lienert, S., Lombardozzi, D., Maki, T., Nakamura, T., Peylin, P., Rödenbeck, C., Zhuravlev, R., Saeki, T., Tian, H., Zhu, D., and Ziehn, T.: State of the science in reconciling top-down and bottom-up approaches for terrestrial CO₂ budget, *Glob. Chang. Biol.*, 26(3), 1068–1084, doi:10.1111/gcb.14917, 2020.
- Konings, A. G., Bloom, A. A., Liu, J., Parazoo, N. C., Schimel, D. S., and Bowman, K. W.: Global, Satellite-Driven Estimates of Heterotrophic Respiration, *Biogeosciences*, 16, 2269–2284, doi:10.5194/bg-2018-466, 2019.
- 1065 Krausmann, F., Erb, K.-H., Gingrich, S., Haberl, H., Bondeau, A., Gaube, V., Lauk, C., Plutzer, C., and Searchinger, T. D.: Global human appropriation of net primary production doubled in the 20th century., *Proc. Natl. Acad. Sci. U. S. A.*, 110(25), 10324–9, doi:10.1073/pnas.1211349110, 2013.
- Kurz, W. A., Dymond, C. C., Stinson, G., Rampley, G. J., Neilson, E. T., Carroll, A. L., Ebata, T., and Safranyik, L.: Mountain pine beetle and forest carbon feedback to climate change, *Nature*, 452(7190), 987–990, doi:10.1038/nature06777, 2008.
- 1070 Lacroix, F., Ilyina, T., and Hartmann, J.: Oceanic CO₂ outgassing and biological production hotspots induced by pre-industrial river loads of nutrients and carbon in a global modeling approach, *Biogeosciences*, 17(1), 55–88, doi:10.5194/bg-17-55-2020, 2020.
- Lauerwald, R., Laruelle, G. G., Hartmann, J., Ciais, P., and Regnier, P. A. G.: Spatial patterns in CO₂ evasion from the global river network. *Global Biogeochem. Cycles*, 29(5). <https://doi.org/10.1002/2014GB004941>, 2015.
- 1075 Li, Y., Piao, S., Li, L. Z. X., Chen, A., Wang, X., Ciais, P., Huang, L., Lian, X., Peng, S., Zeng, Z., Wang, K., and Zhou, L.: Divergent hydrological response to large-scale afforestation and vegetation greening in China, *Sci. Adv.*, 4(5), 1–10, doi:10.1126/sciadv.aar4182, 2018.
- Liang, E., Wang, Y., Piao, S., Lu, X., Camarero, J. J., Zhu, H., Zhu, L., Ellison, A. M., Ciais, P., and Peñuelas, J.: Species interactions slow warming-induced upward shifts of treelines on the Tibetan Plateau, *Proc. Natl. Acad. Sci. U. S. A.*, 113(16), 4380–4385, doi:10.1073/pnas.1520582113, 2016.
- 1080 Liu, J., Baskarran, L., Bowman, K., Schimel, D., Bloom, A. A., Parazoo, N. C., Oda, T., Carroll, D., Menemenlis, D., Joiner, J., Commane, R., Daube, B., Gatti, L. V., McKain, K., Miller, J., Stephens, B. B., Sweeney, C., and Wofsy, S.: Carbon Monitoring System Flux Net Biosphere Exchange 2020 (CMS-Flux NBE 2020). *Earth System Science Data Discussions*, 1–53, 2020.
- 1085 Liu, Y. Y., Van Dijk, A. I. J. M., De Jeu, R. A. M., Canadell, J. G., McCabe, M. F., Evans, J. P., and Wang, G.: Recent reversal in loss of global terrestrial biomass, *Nat. Clim. Chang.*, 5(5), 470–474, doi:10.1038/nclimate2581, 2015.
- Ludwig, W., Amiotte-Suchet, P., Munhoven, G., and Probst, J. L.: Atmospheric CO₂ consumption by continental erosion: Present-day controls and implications for the last glacial maximum, *Glob. Planet. Change*, 16–17, 107–120,



doi:10.1016/S0921-8181(98)00016-2, 1998.

- 1090 Van Der Laan-Luijkx, I. T., Van Der Velde, I. R., Van Der Veen, E., Tsuruta, A., Stanislawska, K., Babenhauserheide, A.,
Fang Zhang, H., Liu, Y., He, W., Chen, H., Masarie, K. A., Krol, M. C., and Peters, W.: The CarbonTracker Data
Assimilation Shell (CTDAS) v1.0: Implementation and global carbon balance 2001-2015, *Geosci. Model Dev.*, 10(7),
2785–2800, doi:10.5194/gmd-10-2785-2017, 2017.
- 1095 Lutz, F., Herzfeld, T., Heinke, J., Rolinski, S., Schaphoff, S., Von Bloh, W., Stoorvogel, J. J., and Müller, C.: Simulating the
effect of tillage practices with the global ecosystem model LPJmL (version 5.0-tillage), *Geosci. Model Dev.*, 12(6),
2419–2440, doi:10.5194/gmd-12-2419-2019, 2019.
- 1100 Luysaert, S., Inglima, I., Jung, M., Richardson, A. D., Reichstein, M., Papale, D., Piao, S. L., Schulze, E. D., Wingate, L.,
Matteucci, G., Aragao, L., Aubinet, M., Beer, C., Bernhofer, C., Black, K. G., Bonal, D., Bonnefond, J. M., Chambers,
J., Ciais, P., Cook, B., Davis, K. J., Dolman, A. J., Gielen, B., Goulden, M., Grace, J., Granier, A., Grelle, A., Griffis,
T., Grünwald, T., Guidolotti, G., Hanson, P. J., Harding, R., Hollinger, D. Y., Hutyrá, L. R., Kolari, P., Kruijt, B., Kutsch,
W., Lagergren, F., Laurila, T., Law, B. E., Le Maire, G., Lindroth, A., Loustau, D., Malhi, Y., Mateus, J., Migliavacca,
M., Misson, L., Montagnani, L., Moncrieff, J., Moors, E., Munger, J. W., Nikinmaa, E., Ollinger, S. V., Pita, G.,
Rebmann, C., Rouspard, O., Saigusa, N., Sanz, M. J., Seufert, G., Sierra, C., Smith, M. L., Tang, J., Valentini, R., Vesala,
T., and Janssens, I. A.: CO₂ balance of boreal, temperate, and tropical forests derived from a global database, *Glob.
Chang. Biol.*, 13(12), 2509–2537, doi:10.1111/j.1365-2486.2007.01439.x, 2007.
- 1105 Luysaert, S., Abril, G., Andres, R., Bastviken, D., Bellassen, V., Bergamaschi, P., Bousquet, P., Chevallier, F., Ciais, P.,
Corazza, M., Dechow, R., Erb, K.-H., Etiope, G., Fortems-Cheiney, A., Grassi, G., Hartmann, J., Jung, M., Lathière, J.,
Lohila, A., Mayorga, E., Moosdorf, N., Njakou, D. S., Otto, J., Papale, D., Peters, W., Peylin, P., Raymond, P.,
Rödenbeck, C., Saarnio, S., Schulze, E.-D., Szopa, S., Thompson, R., Verkerk, P. J., Vuichard, N., Wang, R.,
Wattenbach, M., and Zaehle, S.: The European land and inland water CO₂, CO, CH₄ and N₂O balance between 2001 and
1110 2005, *Biogeosciences*, 9(8), 3357–3380, doi:10.5194/bg-9-3357-2012, 2012.
- Luysaert, S., Marie, G., Valade, A., Chen, Y. Y., Njakou Djomo, S., Ryder, J., Otto, J., Naudts, K., Lansø, A. S., Ghattas, J.,
and McGrath, M. J.: Trade-offs in using European forests to meet climate objectives, *Nature*, 562(7726), 259–262,
doi:10.1038/s41586-018-0577-1, 2018.
- 1115 Maavara, T., Lauerwald, R., Regnier, P., and Van Cappellen, P.: Global perturbation of organic carbon cycling by river
damming, *Nat. Commun.*, 8(1), 15347, doi:10.1038/ncomms15347, 2017.
- MacBean, N., Peylin, P., Chevallier, F., Scholze, M., and Schuermann, G.: Consistent assimilation of multiple data streams in
a carbon cycle data assimilation system, *Geosci. Model Dev.*, 9(10), 3569–3588, 2016.
- Martin, M., Wattenbach, M., Smith, P., Meersmans, J., Jolivet, C., Boulonne, L., and Arrouays, D.: Spatial distribution of soil



- organic carbon stocks in France, *Biogeosciences*, 8(5), 1053–1065, 2011.
- 1120 Mason Earles, J., Yeh, S., and Skog, K. E.: Timing of carbon emissions from global forest clearance, *Nat. Clim. Chang.*, 2(9), 682–685, 2012.
- Mastrandrea, M. D., Mach, K. J., Plattner, G.-K., Edenhofer, O., Stocker, T. F., Field, C. B., Ebi, K. L., and Matschoss, P. R.: The IPCC AR5 guidance note on consistent treatment of uncertainties: a common approach across the working groups, *Clim. Change*, 108(4), 675, 2011.
- 1125 Mayorga, E., Seitzinger, S. P., Harrison, J. A., Dumont, E., Beusen, A. H. W., Bouwman, A. F., Fekete, B. M., Kroeze, C., and Van Drecht, G.: Global nutrient export from WaterSheds 2 (NEWS 2): model development and implementation, *Environ. Model. Softw.*, 25(7), 837–853, 2010.
- Mendonça, R., Müller, R. A., Clow, D., Verpoorter, C., Raymond, P., Tranvik, L. J., and Sobek, S.: Organic carbon burial in global lakes and reservoirs, *Nat. Commun.*, 8(1), 1694, 2017.
- 1130 Mörner, N.-A. and Etiope, G.: Carbon degassing from the lithosphere, *Glob. Planet. Change*, 33(1–2), 185–203, 2002.
- Olin, S., Lindeskog, M., Pugh, T. A. M., Schurgers, G., Wårlind, D., Mishurov, M., Zaehle, S., Stocker, B. D., Smith, B., and Arneeth, A.: Soil carbon management in large-scale Earth system modelling: implications for crop yields and nitrogen leaching, *Earth Syst. Dyn.*, 6(2), 745–768, 2015.
- Olson, R. J., Johnson, K. R., Zheng, D. L., and Scurlock, J. M. O.: Global and regional ecosystem modeling: databases of model drivers and validation measurements, ORNL Technical Memorandum TM-2001/196. Oak Ridge National Laboratory, Oak Ridge, Tennessee, USA., 2001.
- 1135
- Pan, Y., Birdsey, R. A., Fang, J., Houghton, R., Kauppi, P. E., Kurz, W. A., Phillips, O. L., Shvidenko, A., Lewis, S. L., and Canadell, J. G.: A large and persistent carbon sink in the world’s forests, *Science*, 333(6045), 988–993, 2011.
- Peters, G. P., Davis, S. J. and Andrew, R.: A synthesis of carbon in international trade, *Biogeosciences*, 9(8), 3247–3276, doi:10.5194/bg-9-3247-2012, 2012.
- 1140
- Peters, W., Krol, M. C., Van Der Werf, G. R., Houweling, S., Jones, C. D., Hughes, J., Schaefer, K., Masarie, K. A., Jacobson, A. R., and Miller, J. B.: Seven years of recent European net terrestrial carbon dioxide exchange constrained by atmospheric observations, *Glob. Chang. Biol.*, 16(4), 1317–1337, 2010.
- Peylin, P., Law, R. M., Gurney, K. R., Chevallier, F., Jacobson, A. R., Maki, T., Niwa, Y., Patra, P. K., Peters, W., Rayner, P. J., Rödenbeck, C., van der Laan-Luijkx, I. T., and Zhang, X.: Global atmospheric carbon budget: results from an ensemble of atmospheric CO₂ inversions, *Biogeosciences*, 10(10), 6699–6720, doi:10.5194/bg-10-6699-2013, 2013.
- 1145
- Piao, S., Huang, M., Liu, Z., Wang, X., Ciais, P., Canadell, J. G., Wang, K., Bastos, A., Friedlingstein, P., Houghton, R. A., Le Quéré, C., Liu, Y., Myneni, R. B., Peng, S., Pongratz, J., Sitch, S., Yan, T., Wang, Y., Zhu, Z., Wu, D., and Wang,



- 1150 T.: Lower land-use emissions responsible for increased net land carbon sink during the slow warming period, *Nat. Geosci.*, 11(10), 739–743, doi:10.1038/s41561-018-0204-7, 2018.
- Pongratz, J., Reick, C. H., Houghton, R., and House, J.: Terminology as a key uncertainty in net land use and land cover change carbon flux estimates, *Earth Syst. Dyn.*, 5, 177–195, 2014.
- Randerson, J. T., Chapin III, F. S., Harden, J. W., Neff, J. C., & Harmon, M. E. (2002). Net Ecosystem Production : a comprehensive measure of net carbon accumulation by ecosystems *Ecological Applications*, 12(4), 937–947, 2002.
- 1155 Raymond, P. A., Hartmann, J., Lauerwald, R., Sobek, S., McDonald, C., Hoover, M., Butman, D., Striegl, R., Mayorga, E., and Humborg, C.: Global carbon dioxide emissions from inland waters, *Nature*, 503(7476), 355–359, 2013.
- Raymond, P. A., Hartmann, J., Lauerwald, R., Sobek, S., McDonald, C., Hoover, M., Butman, D., Striegl, R., Mayorga, E., and Humborg, C.: Erratum: Global carbon dioxide emissions from inland waters, *Nature*, 507(7492), 387, 2014.
- 1160 Regnier, P., Friedlingstein, P., Ciais, P., Mackenzie, F. T., Gruber, N., Janssens, I. A., Laruelle, G. G., Lauerwald, R., Luyssaert, S., and Andersson, A. J.: Anthropogenic perturbation of the carbon fluxes from land to ocean, *Nat. Geosci.*, 6(8), 597–607, 2013.
- Rödenbeck, C., Houweling, S., Gloor, M., and Heimann, M.: CO₂ flux history 1982–2001 inferred from atmospheric data using a global inversion of atmospheric transport, *Atmos. Chem. Phys.*, 3(6), 1919–1964, doi:10.5194/acp-3-1919-2003, 2003.
- 1165 Running, S. W., Nemani, R. R., Heinsch, F. A., Zhao, M., Reeves, M., and Hashimoto, H.: A continuous satellite-derived measure of global terrestrial primary production, *Bioscience*, 54(6), 547–560, 2004.
- Santoro, M.: GlobBiomass - global datasets of forest biomass, PANGAEA10, 1594, doi:10.1594/PANGAEA.894711, 2018.
- Santoro, M., Kirches, G., Wevers, J., Boettcher, M., Brockmann, C., Lamarche, C., and Defourny, P.: Land Cover CCI Product User Guide Version 2.0, , 1–91, 2017.
- 1170 Saunio, M., Stavert, A. R., Poulter, B., Bousquet, P., Canadell, J. G., Jackson, R. B., Raymond, P. A., Dlugokencky, E. J., Houweling, S., and Patra, P. K.: The global methane budget 2000–2017, *Earth Syst. Sci. data*, 12(3), 1561–1623, 2020.
- Schulze, E.-D., Wirth, C., & Heimann, M. *Managing Forests After Kyoto*. *Science*, 289(5487), 2058–2059, 2000.
- Seinfeld, J. H. and Pandis, S. N.: *Atmospheric Chemistry and Physics: From Air Pollution to Climate Change*, 3rd Edition, Wiley., 2016.
- 1175 Simard, M., Fatoyinbo, L., Smetanka, C., Rivera-Monroy, V. H., Castañeda-Moya, E., Thomas, N., and Van der Stocken, T.: Mangrove canopy height globally related to precipitation, temperature and cyclone frequency, *Nat. Geosci.*, 12(1), 40–45, doi:10.1038/s41561-018-0279-1, 2019.



- 1180 Sindelarova, K., Granier, C., Bouarar, I., Guenther, A., Tilmes, S., Stavrakou, T., Muller, J.-F., Kuhn, U., Stefani, P., and Knorr, W.: Global data set of biogenic VOC emissions calculated by the MEGAN model over the last 30 years, *Atmos. Chem. Phys.*, 14, 9317–9341, doi:10.5194/acp-14-9317-2014, 2014.
- 1185 Sitch, S., Friedlingstein, P., Gruber, N., Jones, S. D., Murray-Tortarolo, G., Ahlström, A., Doney, S. C., Graven, H., Heinze, C., Huntingford, C., Levis, S., Levy, P. E., Lomas, M., Poulter, B., Viovy, N., Zaehle, S., Zeng, N., Arneth, A., Bonan, G., Bopp, L., Canadell, J. G., Chevallier, F., Ciais, P., Ellis, R., Gloor, M., Peylin, P., Piao, S. L., Le Quéré, C., Smith, B., Zhu, Z., and Myneni, R.: Recent trends and drivers of regional sources and sinks of carbon dioxide, *Biogeosciences*, 12(3), 653–679, doi:10.5194/bg-12-653-2015, 2015.
- Song, X.-P., Hansen, M. C., Stehman, S. V., Potapov, P. V., Tyukavina, A., Vermote, E. F., and Townshend, J. R.: Global land change from 1982 to 2016, *Nature*, 560(7720), 639–643, doi:10.1038/s41586-018-0411-9, 2018.
- 1190 Stein, O., Schultz, M. G., Bouarar, I., Clark, H., Huijnen, V., Gaudel, A., George, M., and Clerbaux, C.: On the wintertime low bias of Northern Hemisphere carbon monoxide found in global model simulations, *Atmos. Chem. Phys.*, 14, 9295–9316, 2014.
- Stocker, B. D., Zscheischler, J., Keenan, T. F., Prentice, I. C., Seneviratne, S. I., and Peñuelas, J.: Drought impacts on terrestrial primary production underestimated by satellite monitoring, *Nat. Geosci.*, 12(4), 264–270, doi:10.1038/s41561-019-0318-6, 2019.
- 1195 Suntharalingam, P., Randerson, J. T., Krakauer, N., Logan, J. A., and Jacob, D. J.: Influence of reduced carbon emissions and oxidation on the distribution of atmospheric CO₂: Implications for inversion analyses, *Global Biogeochem. Cycles*, 19(4), 2005.
- Tang, X., Fan, S., Du, M., Zhang, W., Gao, S., Liu, S., Chen, G., Yu, Z., and Yang, W.: Spatial and temporal patterns of global soil heterotrophic respiration in terrestrial ecosystems, *Earth Syst. Sci. Data*, 12(2), 1037–1051, doi:10.5194/essd-12-1037-2020, 2020.
- 1200 Thompson, R. L., Patra, P. K., Chevallier, F., Maksyutov, S., Law, R. M., Ziehn, T., Van der Laan-Luijkx, I. T., Peters, W., Ganshin, A., and Zhuravlev, R.: Top-down assessment of the Asian carbon budget since the mid 1990s, *Nat. Commun.*, 7, 1–10, 2016.
- 1205 Tramontana, G., Jung, M., Schwalm, C. R., Ichii, K., Camps-Valls, G., Ráduly, B., Reichstein, M., Arain, M. A., Cescatti, A., Kiely, G., Merbold, L., Serrano-Ortiz, P., Sickert, S., Wolf, S., and Papale, D.: Predicting carbon dioxide and energy fluxes across global FLUXNET sites with regression algorithms, *Biogeosciences*, 13(14), 4291–4313, doi:10.5194/bg-13-4291-2016, 2016.
- Tum, M., Zeidler, J. N., Günther, K. P., and Esch, T.: Global NPP and straw bioenergy trends for 2000–2014, *Biomass and Bioenergy*, 90, 230–236, doi:https://doi.org/10.1016/j.biombioe.2016.03.040, 2016.



- Warner, D. L., Bond-Lamberty, B., Jian, J., Stell, E., and Vargas, R.: Spatial Predictions and Associated Uncertainty of Annual
1210 Soil Respiration at the Global Scale, *Global Biogeochem. Cycles*, 33(12), 1733–1745, doi:10.1029/2019GB006264,
2019.
- Wei, Y., Liu, S., Huntzinger, D. N., Michalak, A. M., Viovy, N., Post, W. M., Schwalm, C. R., Schaefer, K., Jacobson, A. R.,
Lu, C., Tian, H., Ricciuto, D. M., Cook, R. B., Mao, J., and Shi., X.: NACP MsTMIP: Global and North American Driver
Data for Multi-Model Intercomparison, ORNL Distributed Active Archive Center, Oak Ridge, Tennessee, USA., 2014.
- 1215 van der Werf, G. R., Randerson, J. T., Giglio, L., Collatz, G. J., Mu, M., Kasibhatla, P. S., Morton, D. C., DeFries, R. S., Jin,
Y., and van Leeuwen, T. T.: Global fire emissions and the contribution of deforestation, savanna, forest, agricultural,
and peat fires (1997–2009), *Atmos. Chem. Phys.*, 10(23), 11707–11735, doi:10.5194/acp-10-11707-2010, 2010.
- van der Werf, G. R., Randerson, J. T., Giglio, L., van Leeuwen, T. T., Chen, Y., Rogers, B. M., Mu, M., van Marle, M. J. E.,
Morton, D. C., Collatz, G. J., Yokelson, R. J. and Kasibhatla, P. S.: Global fire emissions estimates during 1997–2016,
1220 *Earth Syst. Sci. Data*, 9(2), 697–720, doi:10.5194/essd-9-697-2017, 2017.
- Williams, C. A., Gu, H., MacLean, R., Masek, J. G., and Collatz, G. J.: Disturbance and the carbon balance of US forests: A
quantitative review of impacts from harvests, fires, insects, and droughts, *Glob. Planet. Change*, 143, 66–80,
doi:https://doi.org/10.1016/j.gloplacha.2016.06.002, 2016.
- Wißkirchen, K., Tum, M., Günther, K. P., Niklaus, M., Eisfelder, C., and Knorr, W.: Quantifying the carbon uptake by
1225 vegetation for Europe on a 1 km² resolution using a remote sensing driven vegetation model, *Geosci. Model Dev.*, 6(5),
1623–1640, doi:10.5194/gmd-6-1623-2013, 2013.
- Wolf, A., Ciais, P., Bellassen, V., Delbart, N., Field, C. B., and Berry, J. A.: Forest biomass allometry in global land surface
models, *Global Biogeochem. Cycles*, 25(3), doi:10.1029/2010GB003917, 2011.
- Yue, C., Ciais, P., Luyssaert, S., Li, W., McGrath, M. J., Chang, J., and Peng, S.: Representing anthropogenic gross land use
1230 change, wood harvest, and forest age dynamics in a global vegetation model ORCHIDEE-MICT v8.4.2, *Geosci. Model
Dev.*, 11(1), 409–428, doi:10.5194/gmd-11-409-2018, 2018.
- Zheng, B., Chevallier, F., Yin, Y., Ciais, P., Fortems-Cheiney, A., Deeter, M. N., Parker, R. J., Wang, Y., Worden, H. M., and
Zhao, Y.: Global atmospheric carbon monoxide budget 2000–2017 inferred from multi-species atmospheric inversions,
Earth Syst. Sci. Data, 11(3), 1411–1436, 2019.
- 1235 Zscheischler, J., Mahecha, M., Reichstein, M., Avitabile, V., Carvalhais, N., Ciais, P., Gans, F., Gruber, N., Hartmann, J.,
Herold, M., Jung, M., Landschützer, P., Laruelle, G., Lauerwald, R., Papale, D., Peylin, P., Regnier, P., Rödenbeck, C.,
Cuesta, R. M. R., and Valentini, R.: Towards an purely data driven view on the global carbon cycle and its spatiotemporal
variability, *EGU General Assembly.*, 2015.



1240 Zscheischler, J., Mahecha, M. D., Avitabile, V., Calle, L., Carvalhais, N., Ciais, P., Gans, F., Gruber, N., Hartmann, J., Herold,
M., Ichii, K., Jung, M., Landschützer, P., Laruelle, G. G., Lauerwald, R., Papale, D., Peylin, P., Poulter, B., Ray, D.,
Regnier, P., Rödenbeck, C., Roman-Cuesta, R. M., Schwalm, C., Tramontana, G., Tyukavina, A., Valentini, R., van
1245 der Werf, G., West, T. O., Wolf, J. E., and Reichstein, M.: Reviews and syntheses: An empirical spatiotemporal
description of the global surface-atmosphere carbon fluxes: opportunities and data limitations, *Biogeosciences*,
14(15), 3685–3703, doi:10.5194/bg-14-3685-2017, 2017.

1245

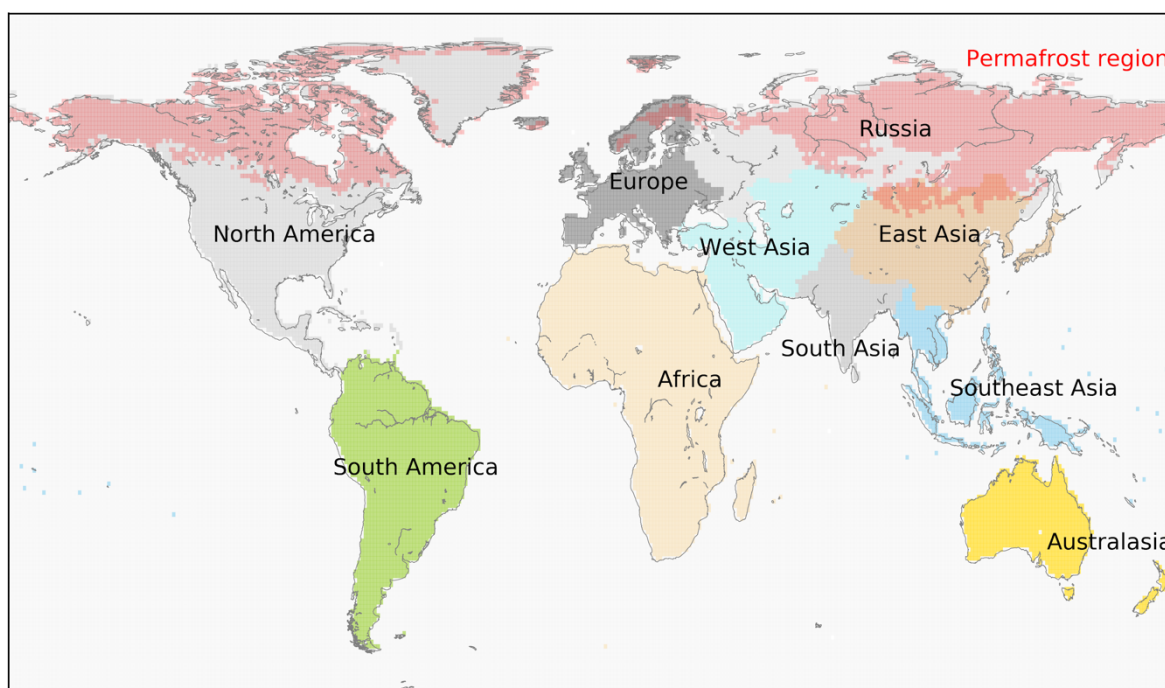
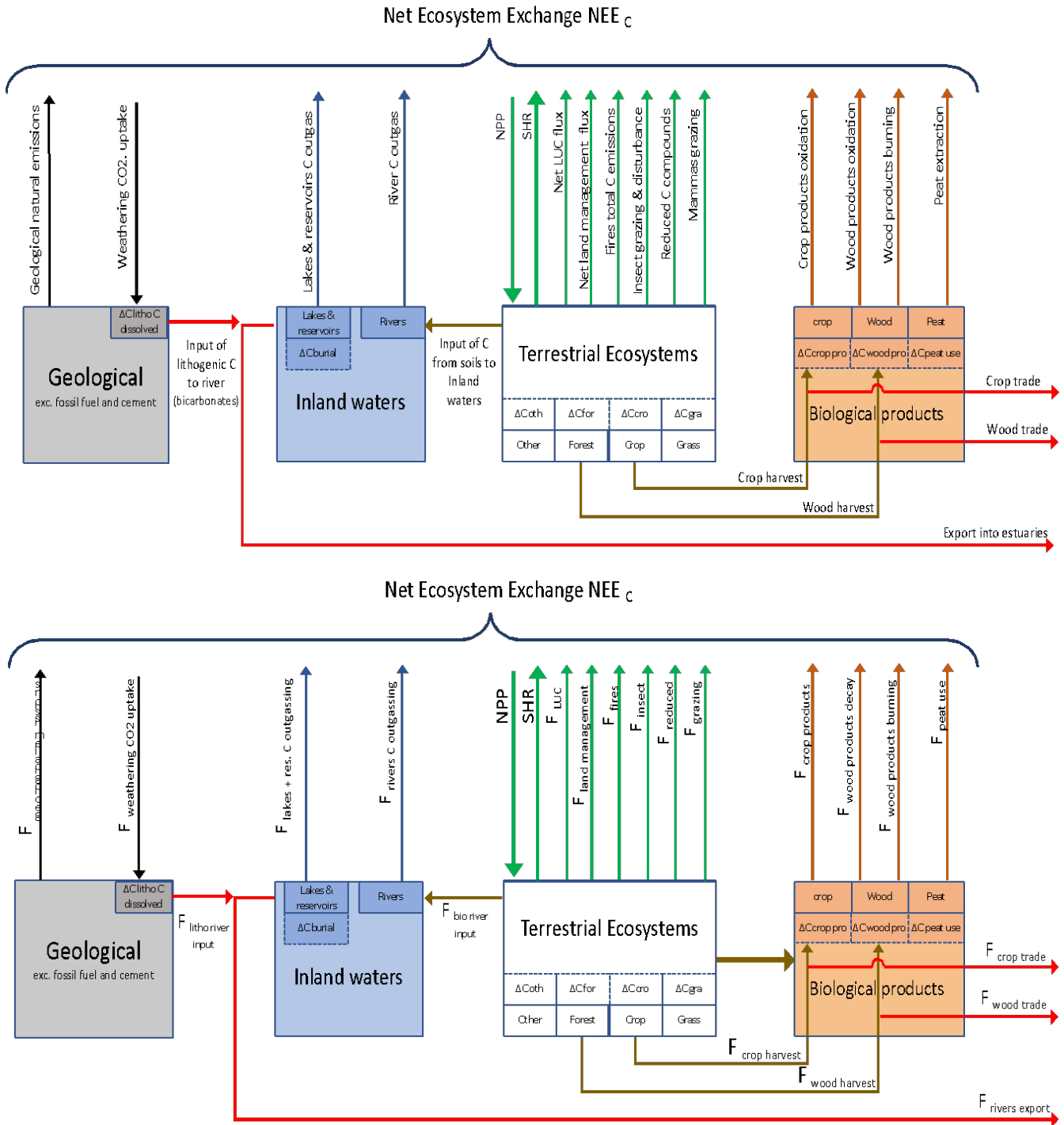
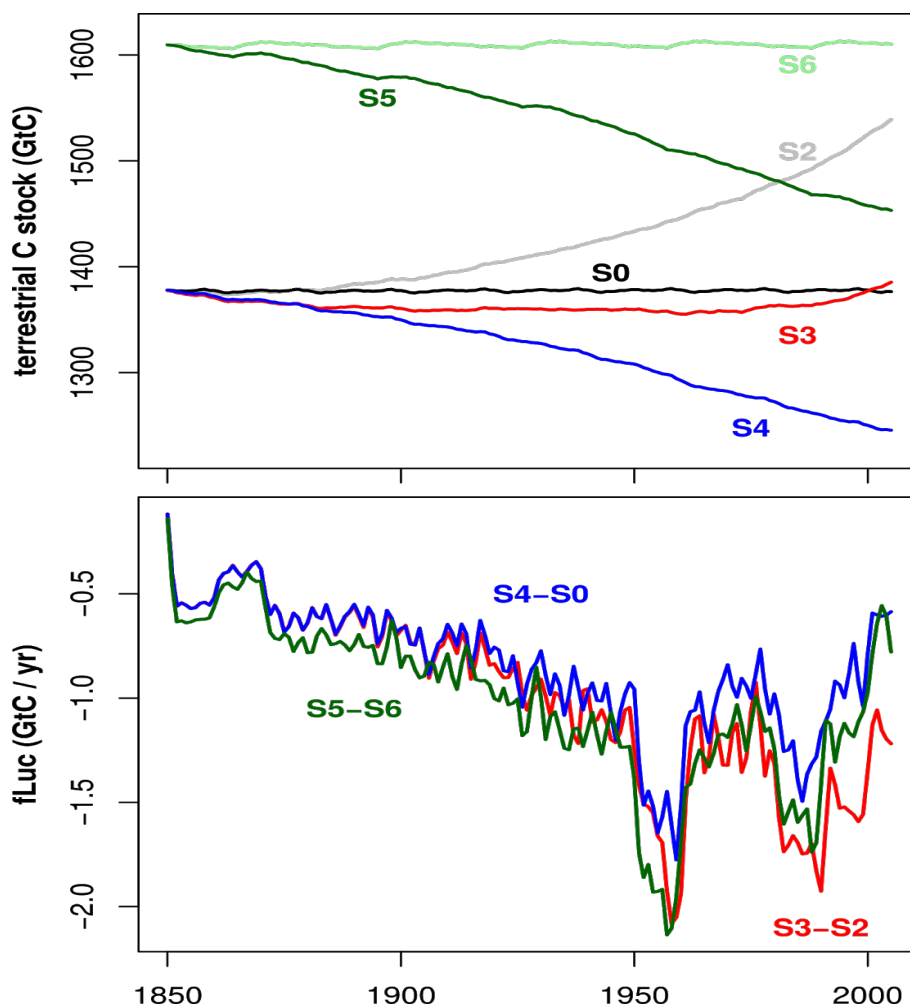


Figure 1: Map of the RECCAP2 regions. The ‘region’ in shaded red corresponds to permafrost covered areas. Map plot
courtesy of Naveen Chandra (NIES/JAMSTEC). Files can be accessed at
1250 https://eocrpa.jamstec.go.jp/~prabir/data/region_masks/RECCAP2_Mask11r.nc
https://eocrpa.jamstec.go.jp/~prabir/data/region_masks/RECCAP2_peramfrost.nc



1255

Figure 2: Summary of C fluxes to be reported in each RECCAP2 region (top) and name of each flux (bottom).



1260 **Figure 3: Terrestrial cumulative C stocks (top) and corresponding F_{LUC} (bottom) as simulated by the JSBACH dynamic vegetation model for the different simulations discussed. Shown is F_{LUC} derived as S5 minus S6, S3 minus S2, and S4 minus S0 (see text).**



Table 1: Main differences between the methods used to estimate F_{LUC} .

Method	C-densities	Transitions	Response of C-stocks	Spatial scale	Period covered	Land use practices included	LASC	Legacy fluxes
H&N Houghton and Nassikas 2017	Present day, aggregated per biome at country-level from FAO	FAOSTAT (2015) data of croplands and pastures areas since 1961. FAO (2015) changes in forest areas since 1990. Data are provided at country-level, and then decomposed per biome based on MODIS IGBP classification (Friedl et al., 2002).	Response curves from literature	Country to global	1850 - 2015	Deforestation; cropland/grassland abandonment; forest degradation; wood harvest; fire suppression (U.S. only); peat drainage and peat burning	No	Yes (for post-1850 LUC)
BLUE	Present day, spatially explicit fields per biome type	Spatially-explicit transitions from LUH2v2 Can be used with RS-based transition maps	Response curves from literature	0.25x0.25 lat. Lon. global coverage Can be adapted to any other spatial resolution if required	850 - present (2018 for Friedlingstein et al., 2019)	Deforestation (separated by transitions to cropland and to grassland); cropland/grassland abandonment; forest degradation; wood harvest; shifting cultivation; peat drainage and peat burning	No	Yes (for post-850 LUC)



DGVMs S3 - S2	Transient (climate + CO ₂)	Spatially-explicit transitions form LUH2v2	Simulated implicitly by DGVMs based on environmental conditions	Model grid scale, global coverage	1700 - present (2018 for Friedlingstein et al., 2019)	Model-dependent (see Friedlingstein et al., 2019 for TRENDY models)	Yes	Yes (for post-1700 LUC)
DGVMs S4 - S0	Pre-industrial (1700) spatially explicit fields Simulated by DGVMs	Spatially-explicit transitions form LUH2v2	Simulated implicitly by DGVMs based on environmental conditions	Model grid scale, global coverage	1700 - present 2018 for Friedlingstein et al., 2019)	Model-dependent (see Friedlingstein et al., 2019 for TRENDY models)	No	Yes (for post-1700 LUC)
DGVMs S5 - S6	Present-day (1999-2018) spatially explicit fields simulated by DGVMs	Spatially-explicit transitions form LUH2v2	Simulated implicitly by DGVMs based on environmental conditions	Model grid scale, global coverage	1700 - present 2018 for Friedlingstein et al., 2019)	Model-dependent (see Friedlingstein et al., 2019 for TRENDY models)	No	Yes (for post-1700 LUC)
RS-based		Changes in LUC derived from RS, e.g. ESA-CCI Land-cover or Hansen et al. (fluxes associated with forest change only)	Estimated by BK or calculated directly from RS-based biomass estimates (e.g. ESA-CCI Biomass product)	Sensor-dependent	Satellite record 1980s -		Yes	Yes (BK) / No (RS only)



Table 2: DGVM simulations to calculate F_{LUC} from TRENDY-v8 protocol (Friedlingstein et al. 2019).

Simulation	Environmental conditions	Land-cover
S0	Time-invariant pre-industrial	Time-invariant pre-industrial
S2	Historic	Time-invariant pre-industrial
S3	Historic	Historic
S4	Time-invariant pre-industrial	Historic
S5	Time-invariant present day	Historic
S6	Time-invariant present day	Time-invariant pre-industrial